SCHOOL OF
PHYSICAL SCIENCES
AND NANOTECHNOLOGY

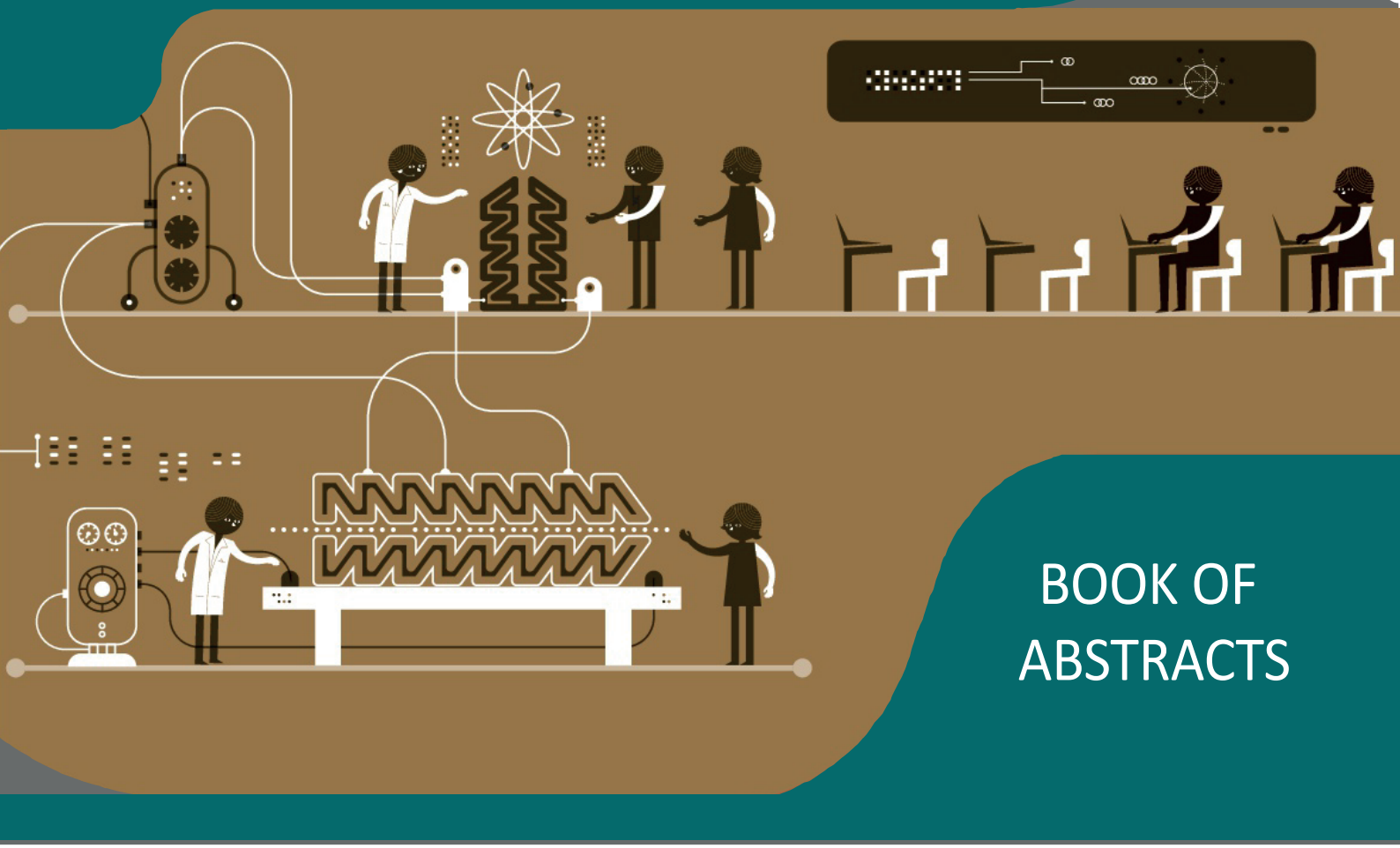

BOOK OF ABSTRACTS

NSSY 2019

Nanoscience Summer School @ Yachay 2019

May, Sunday 26th to June Saturday 1st
Salón de la Ciudad, Santa Cruz
Galápagos-Ecuador

YACHAY TECH

Nanoscience Summer School (NSSY) @ Yachay 2019 International Edition

May 26th to June 1st 2019

SCHOOL OF
PHYSICAL SCIENCES
AND NANOTECHNOLOGY

San Miguel de Urcuquí,
Hacienda San José s/n y Proyecto Yachay
Telephone: +593 6299 9500

Organizing Committee:

Julio Chacón (Chair)
Ernesto Medina
L. Charlotte Berrezueta
Henry Paúl Pinto Esparza
Duncan Mowbray
Camilo Zamora

International Advisory Board:

Damien Voiry
Otakar Frank
Alicja Mikolajczyk
Bakhtiyor Rasulev
Ask Hjorton Larsen
Vito Despoja
Keenan Lyon
Rebeca Ribeiro

Staff:

María José De la Torre
María Rosa Preciado
Romina Bermeo
Jorge Vega

Welcome to NSSY2019

On behalf of The School of Physical Sciences and Nanotechnology at Yachay Tech University in co-operation with the Governing Council of Galapagos, we invite you to join us at the third edition of the Nanoscience Summer School @ Yachay Tech 2019 (NSSY 2019).

The summer school will be held from the 26th of May until the 1st of June 2019 at Puerto Ayora, in the Galapagos Islands, Ecuador. The NSSY 2019 will hold plenary sessions by top international scientists, invited talks from leading researchers in the field, and contributed talks chosen from the best-submitted abstracts. We will also feature a two-day poster sesion, which is a main focus for the program.

In this international edition of NSSY, we anticipate the participation of 120 delegates between speakers, keynotes, professor, researches and Ph.D. and Undergrad Students in an informal atmosphere where they can openly discuss, exchange ideas and results about their latest work in different topics of nanotechnology from both, theoretical and experimental points of views.

Join us at the enchanted venue of the Galapagos archipelago for the NSSY 2019 which is a must-attend for anyone interested in learning about different topics of nanotechnology, their applications, and the most recent discoveries of the field.

See you at the Galapagos islands!

Ernesto Medina, PhD
Dean of the School of Physical Sciences and Nanotechnology at Yachay Tech University

FINAL PROGRAM NSSY 2019

	POLYMER AND BIONANOSCIENCE	THEORY AND SIMULATIONS IN NANOSCIENCE	SYNTHESIS OF NANOMATERIALS	MOLECULAR MODELING OF NANOSTRUCTURES	CHARACTERIZATION OF NANOSTRUCTURES /
	Monday, May 27	**Tuesday, May 28**	**Wednesday, May 29**	**Thursday, May 30**	**Friday, May 31**
8:30 a. m.	Modular Biomimetric Pathways to Enhance Nanodiamond Interface for Bioapplications **MONA JANI**	Computational modelling in nanotoxicology **TOMASZ PUZYN**	Nanomaterials in heterogeneous photocatalysis: from fundamentals to applications **ADRIANA ZALESKA**	Theory and computation in nanoscience **RISTO NIEMINEN**	Raman spectroscopy in carbon nanostructures **ADO JORIO**
9:00 a. m.	Nanosilver in situ synthesis and long term stabilization in vinylacrylic-vinyl- tert-decanoate terpolymer water emulsion **ANTONIO DIAZ**				
9:30 a. m.	Mechanical Deformations and their Influence on the Spin-Orbit Coupling of Chiral-Molecules **SOLMAR VARELA**	Comparison of Empirical Models and Ab initio Calculations with Experiments on Electron Energy Loss Spectroscopy of **ZORAN MISKOVIC**	Tailoring Magnetic SiO2-Mn1-xCoxFe2O4 Nanocomposites Decorated with Au@Fe3O4 Nanoparticles for **SARAH BRICEÑO**	On the nature of the chemical bond in no-pair ferromagnetic metal clusters **LUIS RINCÓN**	Imaging and Spectroscopy of Two Dimensional Graphene Heterostructures **LEONARDO BASILE**
10:00 a. m.	**Coffee Break**	Topological semimetals in external fields **RAFAEL MOLINA**	**Coffee Break**	**Coffee Break**	**Coffee Break**
10:30 a. m.	Nanostructures Based on Block Copolymers **NIKOS HADJICHRISTIDIS**	Conference Tour High side of Santa Cruz (Gemelos/Turtles/Lava cave)	Unprecedented Record on Substitutional B-Doped Single-Walled Carbon Nanotubes **CARLOS REINOSO**	Ab initio study of 2D plasmon enhancement in alkali intercalated graphene on metallic substrates **VITO DESPOJA**	Surface-enhanced spectroscopy and ultra-strong light-matter coupling **STEPHANIE REICH**
11:00 a. m.			Hardness and structural properties of multiwall carbon nanotubes and aluminum-based composites. **ERIC PLAZA**	Two-photon Spectroscopy using Intense Entangled Photon Beams **JIRI SVOZILIK**	
11:30 a. m. . . . 3:00 p. m.	Mini workshops		Mini workshops Charles Darwin Foundation	Mini workshops	Mini workshops
3:30 p. m.				One step synthesis of Fe/Ti oxide nanostructures from Ecuadorian black sands **VICTOR GUERRERO**	Molecular electronic devices based on monomolecular films **HENRY OSORIO**
4:00 p. m.				Driven electronic transport in semi-Dirac materials **ALEXANDER LOPEZ**	Site-controlled Nano-heteroepitaxy of GaAs on Si **IVAN PRIETO**
4:30 p. m.	Using Lignin as a reducing agent for removal of potentially toxic metals **FLORALBA LÓPEZ**			Proximity-induced spin-orbit effects in graphene on Au **MAYRA PERALTA**	Functionalization of Nanostructures: Chemical modification and advanced analysis **CARLA BITTENCOURT**
5:00 p. m.	Natural Fibers with Chemical and Biological Activity **FRANK ALEXIS**			Electron transport simulations of multi-terminal nanoscale devices **THOMAS FREDERIKSEN**	
5:30 p. m.		Dinner		Dinner	Ordering, Instabilities and Textures in Graphene Based Liquid Crystalline phases **CAMILO ZAMORA**
6:00 p. m.	Nano and microplastic pollution of the oceans: today's research for tomorrow's solution **ALONZO NUÑEZ**		Free Time		NSSY 2019 CLOSING TALK **DEAN OF PHYSICS**
6:30 p. m.	Dinner				Closing Dinner
7:00 p. m.			NSSY 2019 Conference Integration Dinner		
7:30 p. m.		Poster Session I		Poster Session II	
8:00 p. m.					
8:30 p. m.	SPECIAL TALK Imaging a Black Hole **JOSE MANUEL** **- SCIENCE CAFEE -**				
9:00 p. m.			**Theater Show**		

Monday

Modular Biomimetric Pathways to Enhance Nanodiamond Interface for Bioapplications

Mona Jani

School of Physical Sciences and Nanotechnology, Yachay Tech University, 100119-Urcuquí, Ecuador

mjani@yachaytech.edu.ec

Fluorescent nanodiamond (nitrogen–vacancy) centers buried inside the core have attracted remarkable scientific attention for applications ranging from bio–imaging to quantum computing. These centers respond to local changes in electric / magnetic fields and do not suffer from photoblinking / photobleaching, which makes nanodiamond a viable platform for long–term imaging processes inside living cells.[1] Lack of commonly followed standard protocols for synthesis and bio interface functionalizations / characterizations, lead to inconsistent results and hinder clinical translation. Thus, small-sized nanodiamonds with a biodegradable, thin, compact polymer coating are anticipated. The presentation will include studies on irradiation methods to produce fluorescent nanodiamonds, approaches to stabilize the dispersion and to reduce the strong non–specific interactions in physiological conditions. Innovative approaches on surface functionalization with PEG or with coating of hydrophilic polymers both by covalent and noncovalent methods without affecting the intrinsic optical properties of the nitrogen-vacancy centers.[2] Emphasis will be given on biointerfacing approaches through modular biomimetric pathways to make them compatible with biological environments for use in biomedical applications.[3] Furthermore, oxygenation–de–oxygenation dynamics and bio–physical interactions focusing on cellular models[4] and merging biocompatibility, modularity, and outstanding spin sensitivity in nanodiamond which provides a foundation for development of multifunctional nanoparticles suitable for highly sensitive monitoring of local magnetic field fluctuations and paramagnetic species under physiological conditions will be presented.

References

[1] Perevedentseva, E.; Lin, Y.-C.; Jani, M.; Cheng, C.-L. *Nanomedicine* **2013**, *8*, 2041–2060.

[2] Pramanik, G.; Neburkova, J.; Vanek, V.; Jani, M.; Kindermann, M.; Cigler, P. *Carbon Nanomaterials for Bioimaging, Bioanalysis, and Therapy* **2019**, 15–42.

[3] Mona, J.; Perevedentseva, E.; Cheng, C.-L. *Nanodiamond*; 2014; pp 170–194.

[4] Vavra, J.; Rehor, I.; Rendler, T.; Jani, M.; Bednar, J.; Baksh, M. M.; Zappe, A.; Wrachtrup, J.; Cigler, P. *Advanced Functional Materials* **2018**, *28*, 1803406.

Nanosilver *in situ* synthesis and long term stabilization in vinylacrylic-vinyl-tert-decanoate terpolymer water emulsion matrix with potential antibacterial applications

Antonio Díaz-Barrios[1]
Gema Gonzalez*[3,4], Jessica Santiana[2], Francisco Quiroz [2], José Iván Chango [2], Cesar Costa Vera [5], Lorenzo Caniglia [6], and Milagro Fernández-Delgado [6]

[1] *School of Chemistry and Engineering Yachay Tech University, Urcuquí.*

[2] *Departamento de Ciencia de los Alimentos y Biotecnología, Escuela Politécnica Nacional Quito, Ecuador*

[3] *School of Physics and Nanotechnology, Yachay Tech University, Urcuquí, Ecuador.*

[4] *Centro de Ingeniería de Materiales y Nanotecnología, Instituto Venezolano de Investigaciones Científicas, Caracas, Venezuela.*

[5] *Departamento de Física, Escuela Politécnica Nacional, Quito, Ecuador.*

[6] *Centro de Biofísica y Bioquímica, Instituto Venezolano de Investigaciones Científicas, Caracas, Venezuela.*

adiaz@yachcaytech.edu.ec*

ggonzalez@yacahytech.edu.ec*

It is of great interest the development of new hybrid materials based on nanosilver (AgNP) and polymers. Several polymers have been used for this purpose.[1–3] However polymeric substrates such as vinylacrylic and derivatives, very well known in industrial applications, have been rarely used for synthesis and stabilization of AgNPs. The purpose of this research is the *in situ* synthesis of AgNP in vinylacrylic-vinyl-tert-decanoate (VAVTD) terpolymer and simultaneously use this polymer as stabilization matrix for the AgNP particles. The corresponding characterization of material was done by UV spectroscopy, SEM and TEM electron microscopy. Preliminary work was carried out to assess the biofilm formation of Pseudomonas aeruginosa on these VAVTD/AgNP hybrids in order to explore their use in antibacterial applications. The results show that VAVTD terpolymer water emulsion is a very good substrate to stabilize AgNP particles as evidenced by the morphologic studies carry out by SEM and TEM and the corresponding UV spectra of AgNP particles, even after 45 d of ageing. It was also found that VAVDT/AgNP composites showed a significant reduction of the cell viability in biofilms ($p<0.05$) at 1 and 7 d, suggesting potential antibacterial properties and potential use for surgery rooms surfaces.

Figure 1. UV Spectra of AgNP particles

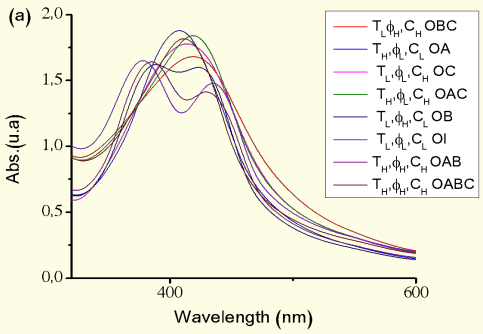

References

[1] Zhang, Z.; Patel, R. C.; Kothari, R.; Johnson, C. P.; Friberg, S. E.; Aikens, P. A. *The Journal of Physical Chemistry B* **2000**, *104*, 1176–1182.

[2] Pencheva, D.; Bryaskova, R.; Kantardjiev, T. *Materials Science and Engineering: C* **2012**, *32*, 2048–2051.

[3] Zhang, Z.; Han, M. *Journal of Materials Chemistry* **2003**, *13*, 641–643.

Mechanical Deformations and their Influence on the Spin-Orbit Coupling of Chiral-Molecules

Solmar Varela[1]
Ernesto Medina, Vladimiro Mujica
[1] *Yachay Tech University. Proyecto Tachay, Hacienda San José. Urcuquí, Ecuador*
svarela@yachaytech.edu.ec solmarvarela@gmail.com

Chiral Induced Spin Selectivity (CISS) consist of the strong spin polarization of electrons when they are transmitted through of chiral molecular structures, including single molecules of DNA, Photosystems, chiral oligopeptides and helicenes. These systems lack strong exchange interactions and magnetic centers, so that it was proposed that the photo- electron spin polarization setup was the spin- orbit (SO) coupling in addition to the chiral potential.[1] The strength of the SO interaction relevant to transport depends critically on the relative geometrical arrangement of current- carrying orbitals. Recent tight-binding orbital models for spin transport in DNA-like molecules, have surmised that the band SO coupling arises from the particular angular relations between orbitals of neighbouring bases on the helical chain.[2] A variety of experimental probes have been developed that result in molecular deformations whose effects have not been addressed in detail.[3,4]

We show that is possible to tune the magnitude of the SO interaction in DNA helix model through changes in the radius and pitch due to the longitudinal deformations.[5] We analyse the behavior of the strength of the SO interaction under effects of longitudinal stretching in two configurations: stretching with a free rotating end, in which the rotation angle between consecutives bases in helix changes, keeping the radius constant; stretching with both ends fixed, with the rotational angle per base is fixed and we assumed the effective elastic behavior like a body with a Poisson ratio (Figure 2). We find that stretching the structure increases the SO coupling by at least 10% in both straining configurations considered, and compressing uniaxially reduces the SO coupling, shown that it is possible manipulate spin active interaction by straining, as it is reported in experiment (Figure 3). We shown that the helicoidal arrangement of the pi-orbitals on the bases is an activating geometry for the SO coupling.

Acknowledgement: This work was supported by grant "CEPRA XII-2108-06 Espectroscopía Mecánica" of CEDIA

Figure 2. Streching with (a) a free rotating end and (b) with both ends fixed.

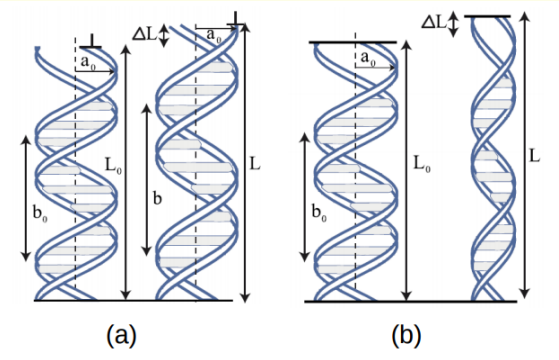

Figure 3. Magnitude of SO coupling versus the strain for the one free end configuration.

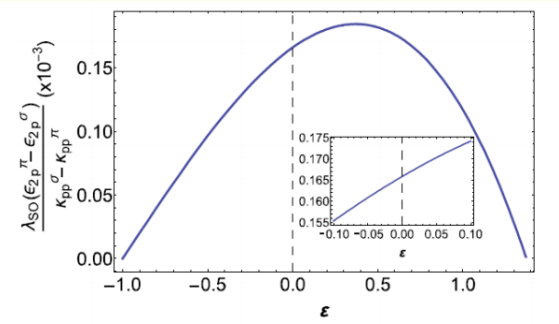

References

[1] Yeganeh, S.; Ratner, M. A.; Medina, E.; Mujica, V. *The Journal of chemical physics* **2009**, *131*, 014707.

[2] Varela, S.; Mujica, V.; Medina, E. *Physical Review B* **2016**, *93*, 155436.

[3] Kiran, V.; Cohen, S. R.; Naaman, R. *The Journal of Chemical Physics* **2017**, *146*, 092302.

[4] Xie, Z.; Markus, T. Z.; Cohen, S. R.; Vager, Z.; Gutierrez, R.; Naaman, R. *Nano Letters* **2011**, *11*, 4652–4655.

[5] Salazar, S. V.; Mujica, V.; Medina, E. *CHIMIA International Journal for Chemistry* **2018**, *72*, 411–417.

Nanostructures Based on Block Copolymers

Nikos Hadjichristidis
King Abdullah University of Science and Technology (KAUST), Saudi Arabia
nikolaos.hadjichristidis@kaust.edu.sa

Linear block copolymers have been the focus of intense basic and technological studies thanks to their ability to self-assemble into well-defined periodic ordered phases on the scale of a few hundred Angstrom. Spherical, cylindrical, bicontinuous, or lamellar morphologies may occur for a given linear block copolymer, depending on the volume fraction of the components. These morphologies give unique properties to block copolymers and until now have led to valuable applications for high-tech nanopatterned materials. In almost all applications, it would be desirable to control the microphase morphology and volume fraction separately. One obvious way to achieve this goal is to change the macromolecular architecture. By applying high vacuum techniques, using anionic polymerization and controlled chlorosilane chemistry, we were able to synthesize a variety of well-defined miktoarm (Greek word $\mu\iota\kappa\tau\zeta$) star block copolymers. The morphology of these novel block copolymers was investigated by TEM, SAXS, and was compared with the corresponding linear. The results clearly show the great control over morphology that can be exerted by manipulating the chain architecture. These controlled morphologies are potential precursors in nanoobject construction. For example, 3D ceramic nanostructured films were produced from silicon-containing block copolymers.

References

[1] Iatrou, H.; Hadjichristidis, N. *Macromolecules* **1993**, *26*, 2479–2484.

[2] Tselikas, Y.; Hadjichristidis, N.; Lescanec, R. L.; Honeker, C. C.; Wohlgemuth, M.; Thomas, E. L. *Macromolecules* **1996**, *29*, 3390–3396.

[3] Tselikas, Y.; Iatrou, H.; Hadjichristidis, N.; Liang, K.; Mohanty, K.; Lohse, D. *The Journal of chemical physics* **1996**, *105*, 2456–2462.

[4] Sioula, S.; Hadjichristidis, N.; Thomas, E. L. *Macromolecules* **1998**, *31*, 5272–5277.

[5] Sioula, S.; Hadjichristidis, N.; Thomas, E. L. *Macromolecules* **1998**, *31*, 8429–8432.

[6] Hadjichristidis, N. *Journal of Polymer Science Part A: Polymer Chemistry* **1999**, *37*, 857–871.

[7] Mavroudis, A.; Avgeropoulos, A.; Hadjichristidis, N.; Thomas, E. L.; Lohse, D. J. *Chemistry of materials* **2003**, *15*, 1976–1983.

[8] Chan, V. Z.-H.; Hoffman, J.; Lee, V. Y.; Iatrou, H.; Avgeropoulos, A.; Hadjichristidis, N.; Miller, R. D.; Thomas, E. L. *Science* **1999**, *286*, 1716–1719.

[9] Hadjichristidis, N.; Pispas, S.; Floudas, G. *Block copolymers: synthetic strategies, physical properties, and applications*; John Wiley & Sons, 2003.

Natural Fibers with Chemical and Biological Activity

Frank Alexis[1,2]
Mery Rosario Ramirez Muñoz[4], Cristóbal Domínguez[4], David García [1], Jenny Antonia Rodriguez León[4], Alexis Debut[3], Salome Galeas [3], Víctor H. Guerrero [5], and Frank Alexis
[1] *School of Biological Sciences and Engineering, Yachay Tech University, Urcuquí, Imbabura, Ecuador*
[2] *BioDiverSource*
[3] *Center of Nanosciences and Nanotechnology, Universidad de las Fuerzas Armadas ESPE, Sangolquí, Ecuador*
[4] *Escuela Superior Politecnica del Litoral, Guayaquil, Ecuador*
[5] *Escuela Politecnica Nacional, Quito, Ecuador*
falexis@yachaytech.edu.ec

The shrimp industry have had a considerable growth over the years, positioning as one of the most important economic income source in many countries around the world. One challenge associated with the shrimp industry is the spreading of diseases that can significantly affect the production yield, one of the most common is the vibriosis. To address this challenge, antibiotics have been used for a long time as a solution to remove this disease but its uncontrolled used have generated a drug resistance to both animals and humans. Currently, the efforts have focused on developing new approaches to prevent production loss by stimulating the immune system of the shrimps. In the present study we demonstrated the immunostimulant properties of natural cellulose fibers incorporated to diet of shrimps. The cellulose fibers were tested in different in vitro and in vivo including a control group. To evaluate the immune response in vitro, we used the anion superoxide test, the phenoloxidase activity test and we performed a hemogram to analyze the amount of hemocytes. Additional in vivo parameters as the amount of protein in plasma and the change weight were also measured juvenile shrimps,before and after 49 days of treatment. The results showed that the juvenile shrimps fed with cellulose increased the activity of the anion superoxide and the phenolixidase, which suggest the stimulation of the immune system. The amount of hemocytes presented a significant difference respect to control group. The weight in juvenile shrimps with treatment showed a little increase respect to the control group. More importantly, more than 80% of the shrimps survived the challenge to vibriosis compared to only 20% of the control group.

Figure 4. SEM images of natural fibers showing differential morphology

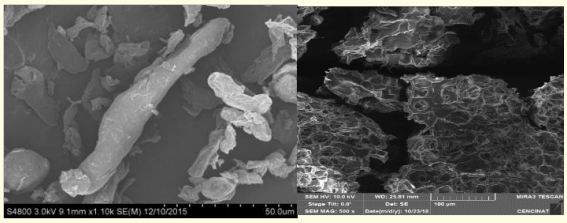

Figure 5. Collection of shrimps for in vivo experiments and preparation of experimental feeds.

Nano and microplastic pollution of the oceans: today's research for tomorrow's solution

Alonzo Alfaro-Núñez[1]

[1] *School of Biological Science and Engineering, Yachay Tech University, 100119 Urcuquí, Ecuador*

aalfaro@yachaytech.edu.ec

Plastic debris degrading into micro and nanoplastic pollution seem particular evident across all ocean environments, appearing as one of the world's main concerns threatening not only the marine wildlife and the ecosystem, but possibly also accumulating in the food chain through ingestion by marine plankton and then moving to higher organisms. Marine food sources support a large part of the world's human protein intake and it is expected that this demand will increase during this century. This main source of human diet is now being threatened by plastic contamination in all ocean environments. We collected water samples across 4000 km trajectory in the Tropical South-Easter Pacific and Galapagos covering an area of 453,000 square kilometers. Moreover, we collected environmental and water samples along the coast and urban areas. Lastly, 98 specimens of 11 different species of fish, squid, and shrimp, all of human consumption were collected along the continental coast in the same sampling area. Microplastic particles were found in 100 % of the water samples and inside of all the marine organisms, confirming that plastic is indisputably ubiquitous. With this project, besides reporting and quantifying the effects of this global problem, we will also attempt to reach three goals. First, we will establish a standardized protocol, a missing gap in this new field of research. Second, we will develop a novel protocol for detection of polymers-plasticizers and persistent organic pollutants (POPs) using methods of Uv/vVis and molecular dyes. And finally, we would characterize cultivable microorganisms with features of naturally biodegrading plastic, and in this way try to propose a potential solution to this global issue.

Imaging a Black Hole

José Ramirez
School of Physical Sciences and Nanotechnology, Yachay Tech University, Urcuquí 100115, Ecuador

jmramirez@yachaytech.edu.ec

In this talk, I will present an overview of the theoretical and observational techniques of the so called "First Photo of a Black Hole", taken by the Event Horizon Telescope (EHT). The challenges and prospectives for the future of this fascinating new view of our Universe will be discussed.

Tuesday

Computational modelling in nanotoxicology

Tomasz Puzyn
Alicja Mikołajczyk, Agnieszka Gajewicz, Ewelina Wyrzykowska, and Maciej Gromelski
Center for Modeling Nano- and Bio-systems, University of Gdansk, Wita Stwosza 63, 80-308 Gdansk, Poland
t.puzyn@qsar.eu.org

Nanotechnology is rapidly growing, and the number of nanomaterials' applications is increasing. But the related enthusiasm needs to be balanced against potential toxicity effects that can be induced by several types of nanoparticles.
Many countries, including the European Union, have introduced specific regulations on the necessary risk assessment procedures for nanoparticles to be performed before introducing new products at the market.
As it is in the case of "classic" chemicals, these regulations recommend applying, whenever possible, alternative methods of the risk assessment. This includes computational modelling techniques that help reducing time, cost and the use of laboratory animals.
However, computational modelling of nanoparticles in the context of nanotoxicology still remains challenging because of several issues. First, nanoparticles are too large systems for calculating structural descriptors in a classical way, from a single molecular model. Second, the nanostructure is not chemically homogenous - it can be considered as an ensemble of different chemical compounds. Third, the nanostructure is labile - changing in time, dependently on the external conditions. Fourth, not only chemistry, but also physics of nanoparticles should be reflected in the models. Finally, the available experimental datasets are limited.
In consequence, seven years after publishing the first Nano-QSAR model,[1] we are coming to the conclusion that many of the initial assumptions on the applicability of classic chemoinformatic paradigms to nanomaterials were overoptimistic.
The lecture will present the state-of-the-art and will discuss most important challenges and further directions of the required research, including possible options for shifting the classic Quantitative Structure-Activity Relationship (QSAR) paradigm to make this type of computational methods more applicable in nanotoxicology.

References

[1] Puzyn, T.; Rasulev, B.; Gajewicz, A.; Hu, X.; Dasari, T. P.; Michalkova, A.; Hwang, H.-M.; Toropov, A.; Leszczynska, D.; Leszczynski, J. *Nature nanotechnology* **2011**, *6*, 175.

Comparison of Empirical Models and Ab initio Calculations with Experiments on Electron Energy Loss Spectroscopy of Graphene

Zoran Miskovic[1]

[1] *Department of Applied Mathematics and Waterloo Institute for Nanotechnology, University of Waterloo, Waterloo, Ontario, Canada*

zmiskovi@uwaterloo.ca

Graphene has come to focus of recent research efforts for applications in plasmonic devices in a broad range of frequencies, from the terahertz (THz) to the far ultraviolet. In that respect, Electron Energy Loss Spectroscopy (EELS) has been recognized as one of the most effective techniques for probing electronic excitations in graphene, both in the low-energy range using High-Resolution Reflection EELS (HREELS) and in the range of energy losses of $\backsim$ 1 – 50 eV using Scanning Transmission Electron Microscopy (STEM).[1]

We have developed a theoretical model for the energy and momentum transfer from an incident charged particle to graphene, treated as a two-dimensional (2D) electron gas characterized by a 2D dynamic conductivity. Initially, this conductivity was modeled using a two-fluid, 2D hydrodynamic (HD) model for the inter-band excitations involving graphene's π and σ electronic bands.[2] This gave very good results in comparison with experiments using HREELS of graphene on metallic substrates for the range of energy losses $\backsim$ 4–10 eV including graphene's π plasmon peak.[3,4] Subsequent applications of the HD model gave excellent comparisons with experimental data for EELS of free-standing graphene in STEM for energy losses $\backsim$ 2–50 eV, which includes both the π and $\sigma + \pi$ peak features of graphene.[5,6]

However, the EELS data for graphene in STEM obtained by different groups revealed intriguing inconsistencies for electron energy losses below some 2–3 eV.[6–8] In order to shed some light on this range of energy losses from a theoretical perspective, we have extended our HD model to low frequencies by adding the so- called Dirac term to the conductivity of graphene.[9] We have further gauged empirical parameters that appear in such extended HD (eHD) model by comparing it with ab initio calculations of the optical conductivity of free- standing graphene.[9,10]

We have further generalized our model of EELS to include retardation effects in the energy losses of a $\backsim$ 100 keV incident electron.[11,12] We have found that the retardation effects play important role at very low energy losses, corresponding to the THz frequency range, where they are found to give rise to significant transition radiation from graphene.[11,12]

References

[1] Politano, A.; Chiarello, G. *Nanoscale* **2014**, *6*, 10927–10940.

[2] Mowbray, D. J.; Segui, S.; Gervasoni, J.; Mišković, Z. L.; Arista, N. R. *Phys. Rev. B* **2010**, *82*, 035405.

[3] Politano, A.; Radović, I.; Borka, D.; Mišković, Z.; Chiarello, G. *Carbon* **2016**, *96*, 91 – 97.

[4] Politano, A.; Radović, I.; Borka, D.; Mišković, Z.; Yu, H.; Farías, D.; Chiarello, G. *Carbon* **2017**, *114*, 70 – 76.

[5] Jovanović, V. B.; Radović, I.; Borka, D.; Mišković, Z. L. *Phys. Rev. B* **2011**, *84*, 155416.

[6] Nelson, F. J.; Idrobo, J.-C.; Fite, J. D.; Mišković, Z. L.; Pennycook, S. J.; Pantelides, S. T.; Lee, J. U.; Diebold, A. C. *Nano Letters* **2014**, *14*, 3827–3831, PMID: 24884760.

[7] Eberlein, T.; Bangert, U.; Nair, R. R.; Jones, R.; Gass, M.; Bleloch, A. L.; Novoselov, K. S.; Geim, A.; Briddon, P. R. *Phys. Rev. B* **2008**, *77*, 233406.

[8] Wachsmuth, P.; Hambach, R.; Kinyanjui, M. K.; Guzzo, M.; Benner, G.; Kaiser, U. *Phys. Rev. B* **2013**, *88*, 075433.

[9] Djordjević, T.; Radović, I.; Despoja, V.; Lyon, K.; Borka, D.; Mišković, Z. L. *Ultramicroscopy* **2018**, *184*, 134 – 142.

[10] Despoja, V.; Djordjević, T.; Karbunar, L.; Radović, I.; Mišković, Z. L. *Phys. Rev. B* **2017**, *96*, 075433.

[11] Mišković, Z. L.; Segui, S.; Gervasoni, J. L.; Arista, N. R. *Phys. Rev. B* **2016**, *94*, 125414.

[12] Akbari, K.; Mišković, Z. L.; Segui, S.; Gervasoni, J. L.; Arista, N. R. *ACS Photonics* **2017**, *4*, 1980.

Topological semimetals in external fields

Rafael A. Molina
J. González, E. Benito-Matías, and Y. Baba
Instituto de Estructura de la Materia (CSIC), Madrid
rafael.molina@csic.es

Topological materials have become a primary target of research in the last few years due to their exceptional properties with high potential for applications. In three dimensions we have the last additions to the family of topological materials, which include Dirac and Weyl semimetals with isolated Dirac or Weyl nodes in the band structure, and the nodal-line semimetals with a continuous line of nodes in the Brillouin zone. The surface states corresponding to these topological semimetals lie on constant energy contours which do not form closed curves. We study the properties of topological semimetals in external electric and magnetic fields. First, we investigate the topological protection of surface states in Weyl, Dirac, and nodal-line semimetals by characterizing them as evanescent states when the band structure is extended to complex momenta.[1] Analytical formulas for the description of these surface states are provided.[2] These formulae can be used in the description of the effects of external electric fields both dc and ac and magnetic fields. In the presence of circularly polarized electromagnetic radiation new surface states develop in topological semimetals which decay from the surface exposed to the radiation and carry angular current (Fig.6). These states should manifest in the observation of a macroscopic chirac current in the irradiated surface.[3] We also show that, under a strong magnetic field, a 3D nodal-line semimetal is driven into a topological insulating phase in which the electronic transport takes place at the surface of the material. Depending on whether the magnetic field is perpendicular or parallel to the nodal ring we obtain a 2D surface quantum Hall effect or a 3D quantum Hall effect with flat level Landau states residing in parallel 2D slices of the 3D material. The Hall conductance is quantized in either case in units of e^2/h and in the 3D Hall effect the number of channels grows with the section of the surface leading to a macroscopic chiral current in the surface of the material.

Figure 6. Probability distribution of the evanescent states along the radial direction (left), time-depending angular current for the upper and middle states of the left part (right).

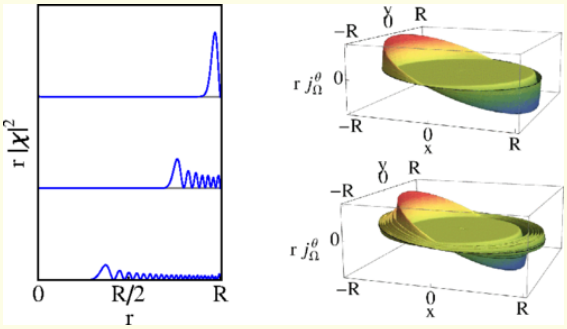

References

[1] González, J.; Molina, R. *Physical Review B* **2017**, *96*, 045437.

[2] Benito-Matías, E.; Molina, R. A. *Physical Review B* **2019**, *99*, 075304.

[3] González, J.; Molina, R. A. *Physical review letters* **2016**, *116*, 156803.

[4] Molina, R. A.; González, J. *Physical review letters* **2018**, *120*, 146601.

Poster Session One

Ni doped Cu-BTC based materials for CO2 adsorption and catalysis

Jeremee Zenteno

Thibault Terencio, and Sandra Leora-Serna
University Yachay Tech, Yachay City of Knowledge,Urcuqui, Ecuador
UAM Azcapotzalco, Ciudad de México, Mexico
jeremee.zenteno@yachaytech.edu.ec

Metal organic frameworks (MOF) are novel materials with huge application such as catalysis, dye adsorption, drug retention or gas storage.[1,2] In fact, MOFs have the ability to retain molecules inside their micro porosity or onto its surface due to its 3D structure. One of the main advantage of the MOFs is the chemical diversity present at their surface due to the fact that they consist of an organic ligand and a metal center. In our case, copper(II) acts as the metal center and benzene-1, 3, 5 tricarboxylic acid (BTC) as organic ligand, to form HKUST-1 (CuBTC). Despite the diversity of existing inorganic and organic parts, each MOF contains usually only one type of transition metal. However, the advantage of having two different metals brings usually new properties, as for example in the case of CuNi alloys. The objective of this work is to take advantage of two different metals, namely copper and Nickel, and the 3D structure of the MOF. Or, in other words make Ni-doping of the HKUST-1 material, verified both by experimental and theoretical technics. And, finally, test the catalytic activity of this new material. The first part of this work was dedicated to the synthesis of the MOF HKUST-1 using “metathesis” method as alternative to the most common solvothermal approach.[3] This material was characterized by XRD compared to literature, DFT simulation, SEM and UV-vis. The second part of this work was focused on the doping of MOF with nanoparticles (NP) of nickel by two methods: direct impregnation and in-situ (one-step). The coordinated water in HKUST-1 are easily removed by thermal treatment at certain temperature (ca 200 C) leaving the Cu(II) sites open, acting as Lewis acid sites. The possibility of doing this pre-activation before doping was also probed. The obtained materials were characterized with UV-Vis and Near infrared (NIR) spectroscopy in order to evaluate the success of Ni-doping. Experimental data is compared to DFT simulations using a representative cluster of the MOF HKUST-1 (Paddlewheel) and the possible materials obtained either with the substitution of one or two copper atoms by nickel atom.(Figure 1) Apart from the metal center, the positioning of nickel nanoparticles in the pores of MOF is discussed. Nickel nanoparticles immobilized into MOF show to be active catalysts in the hydrogenation process such as alkynes, aromatics, alkenes, ketones, and other substrates.[4] The third part of this work is focused on two catalytic tests of the obtained material due to the importance of their products such as alkanes, CO, and hydrogen in petrochemical industry. The two proposed reactions with Nickel doped HKUST-1 are: first, DRM (Dry Reforming Methane) catalytic reaction that utilizes two Greenhouse gases CH_4 and CO_2 to produce syngas, and second hydrogenation of alkenes.[5] Their activity is compared to the non-modified Cu-BTC in order to evaluate the advantage of Ni-doping such material.

Figure 7. View of paddlewheel cluster and the problem of Ni position

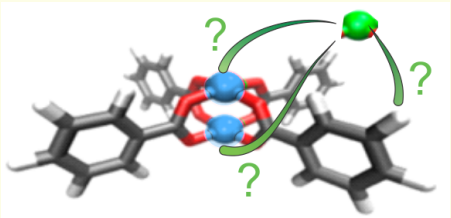

References

[1] Lee, J.; Farha, O. K.; Roberts, J.; Scheidt, K. A.; Nguyen, S. T.; Hupp, J. T. *Chemical Society Reviews* **2009**, *38*, 1450.

[2] International Journal of Environmental Science and Development. https://doi.org/10.18178/ijesd.

[3] Safii, F. F.; Ediati, R. *IPTEK Journal of Proceedings Series* **2016**, *2*.

[4] Xiang, W.; Zhang, Y.; Lin, H.; jun Liu, C. *Molecules* **2017**, *22*, 2103.

[5] Wang, Y.; Yao, L.; Wang, S.; Mao, D.; Hu, C. *Fuel Processing Technology* **2018**, *169*, 199–206.

Controlled synthesis of silver nanoplates: a photochemical approach

José A. Arcos-Pareja[1]
Esteban D. Lasso, Synei Benalcázar J., Sarah Briceño, and Julio C. Chacón-Torres
Yachay Tech University, School of Physical Sciences and Nanotechnology, Urcuquí 100119, Ecuador
jose.arcos@yachaytech.edu.ec

Triangular silver nanoplates(SNPs) are interesting structures that show controllable optical, antibacterial and catalytic properties.[1] The size and shape of these nanostructures strongly depend on their length, size, thickness and the termination of their edges (tips).[2] The photochemical approach, which is among the synthesis methods, is considered the most facile and simple technique to synthesize and control the shape of those SNPs.[3] This method requires only a few chemical reagents and light emission diodes (LEDs), which provides high control on the size of the SNPs since the LEDs' wavelength used in the synthesis is directly related to the size of the samples.[3] On the other hand, a concern with the photochemical synthesis is the low conversion rate from spherical to triangular plates (70%). This rate can be improved by the addition of H_2O_2 that acts as an etching agent,[2] regulating the photoconversion process and considerably improving the conversion rate and reaction time. In this work we compare different methods and develop a different optimized one to synthesize SPNs. UV-vis spectroscopy and (Transmission Electron Microscopy) TEM images will serve as tools to define the homogeneity and quality of the final SNPs. As a final outcome, a comprehensive understanding of the SNPs mechanism will be given including the role of each chemical reagent, specifically H_2O_2 conversion. Figure 1 shows UV-vis spectrum of Ag SNPs where we can see an improvement at the 330 nm, 400 nm and 510 nm resonances, indicating an improvement in quality of the sample.

Figure 8. UV-vis spectra of Ag SNPs synthesized by different methods. The different plasmonic resonances can be observed as indicators of quality.

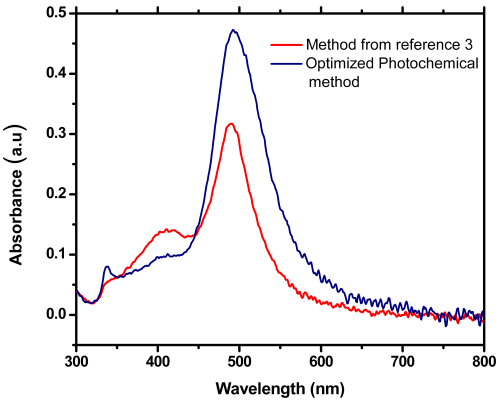

References

[1] Zhang, J.; Langille, M. R.; Mirkin, C. A. *Journal of the American Chemical Society* **2010**, *132*, 12502–12510.

[2] Zhang, Q.; Li, N.; Goebl, J.; Lu, Z.; Yin, Y. *Journal of the American Chemical Society* **2011**, *133*, 18931–18939.

[3] Saade, J.; de Araújo, C. B. *Materials Chemistry and Physics* **2014**, *148*, 1184–1193.

Zirconia doped carbon nanotubes a nanostructured system for biosensor applications

Marlon Danny Jerez-Masaquiza[1]
Gema González Vásquez[1,2], and Mayra Alejandra de Jesús Peralta Arcia[1]
[1] *School of Physical Sciences and Nanotechnology, Yachay Tech University, Urcuqui, Ecuador*
[2] *Instituto Venezolano de Investigaciones Científicas (IVIC), Apartado 20632, Caracas 1020-A, Venezuela*
marlon.jerez@yachaytech.edu.ec

The electrochemical characteristics of a zirconia nanoparticles (NPs) doped multiwall carbon nanotubes-based biosensor for glucose detection are studied. Previous researches suggest that combination of NPs and multiwall carbon nanotubes (MWCNTs) will have a synergistic effect, since both elements, on themselves present important biosensing properties. Wei M. and Tian D. developed a biosensor based on ZnO-MWCNTs/Nafion. They show that the biosensor has high stability and high catalytic activity to H_2O_2, and they conclude this type of combination can provide a good electrochemical sensing platform for redox proteins.[1] Furthermore, the electronic interaction between CNTs and NPs will be studied by using tightbinding model. Yoshioka, T., Suzuura, H., & Ando, T. studied the boron carbonitrate alloy nanotubes. They found that B-N atoms can be regarded as scatterers and contribute mainly to the broadening of the density of states when their concentration is low.[2]
The electrochemical characterization was carried out in a AutoLab potentiostat. Cyclic voltammetry (CV), chronoamperometry (CA) and electrochemical impedance spectroscopy (EIS) techniques were used. Moreover, nanomaterials were structurally characterized by TEM, SEM, XRD, DSC, TGA, FTIR, and Raman.
Keywords: Analytical chemistry, electrochemistry, biosensor, carbon nanotubes, glucose, glucose oxidase.

Figure 9. Glucose detection mechanism using Zirconia doped MWCNTs-modified electrode

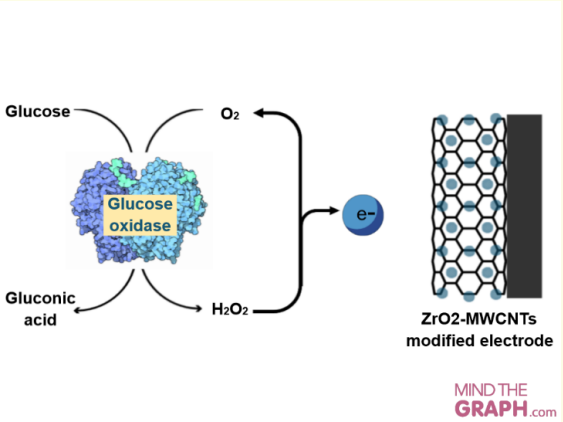

References

[1] Ma, W.; Tian, D. *Bioelectrochemistry* **2010**, *78*, 106–112.

[2] Yoshioka, T.; Suzuura, H.; Ando, T. *Journal of the Physical Society of Japan* **2003**, *72*, 2656–2664.

Removal of zinc using a magnetite-reduced graphene oxide composite

Bryan Alejandro Morillo[1]
Nicole Garcés, María Belén Aldás, Víctor H. Guerrero, and Cristina E. Almeida-Naranjo
Escuela Politécnica Nacional, Ladrón de Guevara E11-253, Quito, Ecuador
bryan.morillo@epn.edu.ec

The industrial wastewater (IWW) discharge produces negative effects to ecosystems and human health, due to the toxicity of the pollutants found. These pollutants include heavy metals, which in several cases are present in relatively high concentrations (20.4 to 93.2 ppm) [1]. One of the most common heavy metals observed is zinc (Zn), which is widely used in a variety of industrial applications (13 million tons of Zn yearly) [2]. There are several different ways to remove Zn from wastewater, including filtration, reverse osmosis, and electrocoagulation [3]. However, these methods have problems associated to high maintenance costs and energy consumption, design limitations and incomplete removal of pollutants during wastewater treatment [4]. Adsorption using activated carbon is another alternative to remove Zn. However, the use of novel adsorbents is one of the most promising methods to remove heavy metals due to their low cost, high efficiency, and wide adaptability. Nanomaterials (zeolites, carbon nanotubes, iron oxides, graphene oxide, among others) and composites are among the highly efficient materials [3].
The aim of this work was to evaluate the adsorption capacity of magnetite-reduced graphene oxide composites (M-RGO) to remove zinc from synthetic water using batch tests. The adsorption tests were carried out considering as variables the contact time, adsorbent dosage and pollutant concentration. Reduced graphene oxide (RGO) was synthesized by the Marcano improved method [5], using a solution of sulfuric acid and phosphoric acid, in a 9:1 ratio. Ultrasonication was used to exfoliate the graphene oxide. M-RGO composites were obtained by co-precipitation [6] using three different mass ratios: 1:2, 1:1 and 2:1. Raman spectroscopy, scanning electron microscopy (SEM), Fourier transform infrared spectroscopy (FTIR) and Brunauer, Emmett and Teller (BET) techniques were used to study the structure, morphology, functional groups and porosity of the composites [5-7]. The M-RGO composites were used in batch adsorption tests [8] in which the Zn concentration was quantified by atomic absorption spectroscopy. The Zn removal from synthetic waters using these composites reached up to approximately 99 % depending on the testing conditions.

References

[1] Al-Shannag, M.; Al-Qodah, Z.; Bani-Melhem, K.; Qtaishat, M. R.; Alkasrawi, M. *Chemical Engineering Journal* **2015**, *260*, 749–756.

[2] Kim, B.-K.; Lee, E. J.; Kang, Y.; Lee, J.-J. *Journal of Industrial and Engineering Chemistry* **2018**, *61*, 388–397.

[3] Liu, M.; Chen, C.; Hu, J.; Wu, X.; Wang, X. *The Journal of Physical Chemistry C* **2011**, *115*, 25234–25240.

[4] Luo, Y.; Guo, W.; Ngo, H. H.; Nghiem, L. D.; Hai, F. I.; Zhang, J.; Liang, S.; Wang, X. C. *Science of The Total Environment* **2014**, *473-474*, 619–641.

[5] Marcano, D. C.; Kosynkin, D. V.; Berlin, J. M.; Sinitskii, A.; Sun, Z.; Slesarev, A.; Alemany, L. B.; Lu, W.; Tour, J. M. *ACS Nano* **2010**, *4*, 4806–4814.

[6] Ge, R.; Liu, C.; Zhang, X.; Wang, W.; Li, B.; Liu, J.; Liu, Y.; Sun, H.; Zhang, D.; Hou, Y.; Zhang, H.; Yang, B. *ACS Applied Materials & Interfaces* **2018**, *10*, 20342–20355.

[7] Tang, Y.; Guo, H.; Xiao, L.; Yu, S.; Gao, N.; Wang, Y. *Colloids and Surfaces A: Physicochemical and Engineering Aspects* **2013**, *424*, 74–80.

[8] Luo, X.; Wang, C.; Luo, S.; Dong, R.; Tu, X.; Zeng, G. *Chemical Engineering Journal* **2012**, *187*, 45–52.

Titanate nanotube/$Al_2W_3O_{12}$/epoxy ternary composites with reduced thermal expansion

Alex Tamayo[1]
Karina Lagos[1], Marco V. Guamán[2], Víctor H. Guerrero [1], Bojan A. Marinkovic[3], and Patricia I. Pontón[1]
[1] *Department of Materials, Escuela Politécnica Nacional, 170525, Quito, Ecuador*
[2] *Department of Mechanical Engineering, Escuela Politécnica Nacional, 170525, Quito, Ecuador*
[3] *Department of Chemical and Materials Engineering, Pontifical Catholic University of Rio de Janeiro, 22451-900, Rio de Janeiro, RJ, Brazil*
alex.tamayo@epn.edu.ec

Epoxy resins are widely used in different engineering fields due to their high elastic modulus, low density, chemical resistance and convenient processing. However, they exhibit a large coefficient of thermal expansion (CTE), ranging between 40-80x10−6 ° C^{-1}, which causes poor dimensional stability under temperature variations.[1] This restrains their use in electronic and aerospace devices, submarine and building coatings, i.e., applications involving direct contact with metal or ceramic substrates, which have lower CTEs. This CTE mismatch can cause thermal stresses at the interface and provoke failure of the polymer component. An inspiring approach to decrease the CTE of epoxy is the addition of thermomiotic-like fillers. Hence, ceramics from $A_2M_3O_{12}$ family, exhibiting low, negative or near zero thermal expansion, such as $Al_2W_3O_{12}$ (CTE ~ 1.75x10^{-6} ° C^{-1}), are deemed as ideal candidates. However, the bulk and Young's moduli of $Al_2W_3O_{12}$ are lower compared with traditional engineering ceramics. Since the CTE of composites not depends solely on the CTE of their components, their volume fraction and the dispersion state of the filler, but also on their bulk moduli (which are function of the stiffness), the addition of a second stiffer filler, creating a hybrid filler, can counteract this disadvantage. Thus, 1D layered nanostructures with large surface area, such as titanate nanotubes (TTNT), synthesized by an inexpensive alkaline hydrothermal treatment, can be considered as a viable choice.[2] In this context, the aim of this study is to prepare epoxy composites reinforced with TTNT/$Al_2W_3O_{12}$ hybrid filler to reduce the CTE of the matrix without causing a significant gain in weight. The matrix consisted of EPON 828 resin and diethylenetriamine (DETA), as a hardener (mass ratio of 100:12). The hybrid filler was added in 0.02 and 0.04 mass fractions with the TTNT/$Al_2W_3O_{12}$ mass ratio of 2:1. An ultrasonic probe was used to disperse the fillers into EPON 828. The composites were casted into silicon molds, cured at room temperature and then post-cure at 80 °C for 24 h. Thermomechanical analysis (TMA) were performed to determine the glass transition temperature (T_g) of the as-prepared composites and their CTE, before and after Tg. This analysis was crucial to demonstrate that extremely low amounts of TTNT/$Al_2W_3O_{12}$ hybrid filler allow the decrease of the CTE of epoxy without negatively affecting its mechanical properties, as confirmed by tensile test.

Figure 10. Procedure to prepare epoxy-based composites reinforced with TTNT/$Al_2W_3O_{12}$ hybrid filler.

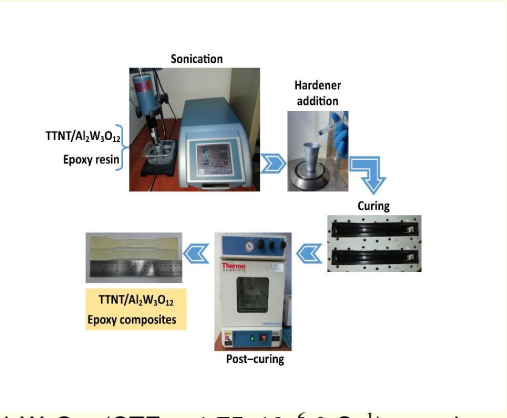

References

[1] Huang, R.; Chen, Z.; Chu, X.; Wu, Z.; Li, L. *Journal of Composite Materials* **2011**, *45*, 1675–1682.

[2] Pontón, P. I.; Yamada, K.; Guamán, M. V.; Johnson, M. B.; White, M. A.; Pandoli, O.; Costa, A. M.; Marinkovic, B. A. *Materials Today Communications* **2019**, *18*, 124–135.

Removal of caffeine with magnetite and oxide graphene

Nicole B. Garcés-Guamba
Bryan A. Morillo, María Belén Aldás, Víctor H. Guerrero, and Cristina E. Almeida Naranjo
Escuela Politécnica Nacional, Ladrón de Guevara E11-253, Quito, Ecuador
nicole.garces@epn.edu.ec

The use of Emerging Pollutants (EPs) such as pharmaceuticals and personal care products, pesticides, endocrine disruptors, illicit drugs and others, have been increased through the last years. EPs are introduced in the ecosystem after being consumed or excreted through feces and urine.[1] EPs cannot be removed by conventional processes and as a result of this EPs are dumped into water resources, increasing the pollution load of the wastewater.[2] One of the most used EPs is the caffeine (1,3,7-trimethylpurine-2,6-dione, CAF) that is present in more than 60 natural products and is used as stimulant in foods and pharmaceutic products.[3] Caffeine in higher concentration produce adverse effect in human health such as tachycardia, insomnia, edginess, nephropathy, gastric upset and psychiatric issues.[4] Due to its high use, caffeine has been found in different water resources, in concentration of 5,597 ± 5,077 ng L^{-1}.[5] In the search of new technologies to remove caffeine from wastewater, the adsorption method has become the most preferred due to its low cost, high efficiency and many adsorbent materials such as activated carbon, polymer and nanomaterials.[6] Magnetite (MNP) and graphene oxide (GO) are useful adsorbent to remove pollutants because they present higher removal efficiency (between 90% to 98%).[7,8] The aim of this study is to compare the removal of caffeine with nanoparticles of magnetite and reduced graphene oxide. GO was synthesized by Hummers improved method using the reaction of sulfuric acid and phosphoric acid in a 9:1 mixture and potassium manganate (VII). This method does not generate toxic gas.[8] MNP was synthesized through chemistry coprecipitation of ferrous (Fe^{+2}) and ferric (Fe^{3+}) ions in alkaline medium.[8] The nanoparticles were characterized by scanning electron microscopy (SEM), X-ray diffraction (XDR), Fourier-transform infrared spectroscopy (FTIR) and Brunauer-Emmett-Teller (BET).[9,10] The analysis of the CAF adsorption was done by batch experiments, which were conducted by triplicated.[10] The results of the adsorption process of the CAF will be exposed in the conference of NSSY 2019, and it is expected that this experiment has higher removal efficiency and establish the best nano adsorbent between GO and MNP.

Figure 11. Procedure to prepare epoxy-based composites reinforced with TTNT/$Al_2W_3O_{12}$ hybrid filler.

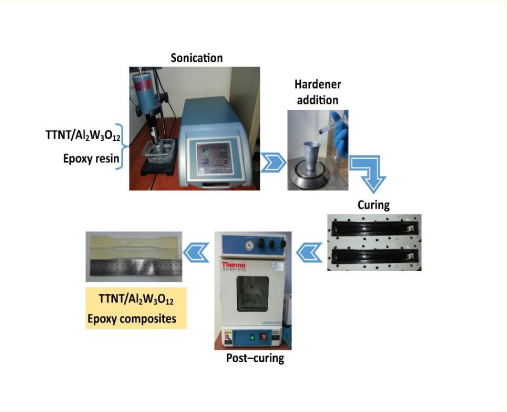

References

[1] Banjac, Z.; Ginebreda, A.; Kuzmanovic, M.; Marcé, R.; Nadal, M.; Riera, J. M.; Barceló, D. *Science of the Total Environment* **2015**, *520*, 241–252.

[2] Luo, Y.; Guo, W.; Ngo, H. H.; Nghiem, L. D.; Hai, F. I.; Zhang, J.; Liang, S.; Wang, X. C. *Science of the total environment* **2014**, *473*, 619–641.

[3] others„ et al. *Environment international* **2017**, *99*, 131–150.

[4] Lozano, R. P.; García, Y. A.; Tafalla, D. B.; Albaladejo, M. F. *Adicciones* **2007**, *19*, 225.

[5] Voloshenko-Rossin, A.; Gasser, G.; Cohen, K.; Gun, J.; Cumbal-Flores, L.; Parra-Morales, W.; Sarabia, F.; Ojeda, F.; Lev, O. *Environmental Science: Processes & Impacts* **2015**, *17*, 41–53.

[6] Boudrahem, F.; Aissani-Benissad, F.; Aït-Amar, H. *Journal of environmental management* **2009**, *90*, 3031–3039.

[7] Cruz, E.; R., M.; Jimenez, J.; Díaz, S.; Calderón, F. *Revista Cubana de Física* **2011)**, *31*, 77–78.

[8] Zhao, G.; Ren, X.; Gao, X.; Tan, X.; Li, J.; Chen, C.; Huang, Y.; Wang, X. *Dalton Transactions* **2011**, *40*, 10945–10952.

[9] Marcano, D. C.; Kosynkin, D. V.; Berlin, J. M.; Sinitskii, A.; Sun, Z.; Slesarev, A.; Alemany, L. B.; Lu, W.; Tour, J. M. *ACS nano* **2010**, *4*, 4806–4814.

[10] Sun, S.; Zeng, H. *Journal of the American Chemical Society* **2002**, *124*, 8204–8205.

Synthesis of magnetic nanoparticles and study of the variation in coactivity field as a function of proportion between single domains (SD) to superparamagnetic (SP) nanoparticles

Kevin R. Landázuri
Werner B. Escamila, and Sarah E. Briceño
Yachay Tech University, Urcuqui, Imbabura, Ecuador
kevin.landazuri@yachaytech.edu.ec

The subsequent thesis project presents a synthesis of magnetite nanoparticles Fe_3O_4 by controlled time reaction co-precipitation method, its magnetic properties as a function of size particle are studied, the resulting hysteresis loops presents behaviour as middle-flattened (wasp-waisted loops) and slouching shoulders (pot-bellies), due to a mixture of population between Single Domain (SD) and Superparmagnetic (SP) grains, to raise either SD and SP magnetic behaviour is needed to vary the size particle of nanoparticles, consequently the size particle is partially controlled by the reaction time in the co-precipitation process. The characterization involves techniques as: SEM and XRD, to get the structural composition and VSM to study the magnetic properties, SEM and VSM will be available on Yachay Tech, whereas XRD should need a research support. The variation on the magnetic properties is widely studied in the field of magnetic-recording devices or nano-devices in an electronic-magnetic component.

Figure 12. (a), (b), and (c) Representative hysteresis loops reported from submarine basaltic glasses.[1]

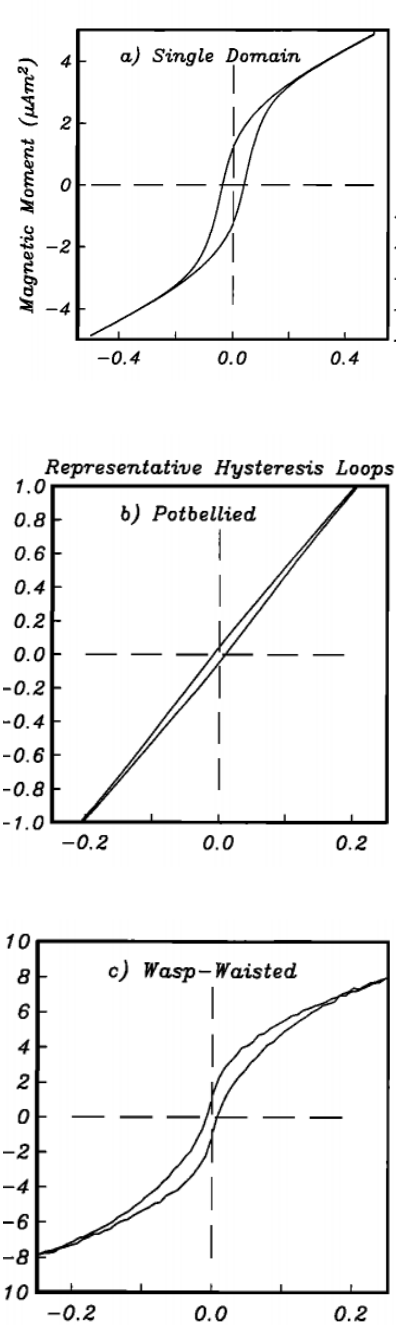

References

[1] Tauxe, L.; Mullender, T. A. T.; Pick, T. *Journal of Geophysical Research: Solid Earth* **1996**, *101*, 571–583.

Characterization of a Homogeneous Dispersed Kaolinite/Carbon Nanotubes Nanocomposite

Vanessa Hinojosa
Julio C. Chacón-Torres
Yachay Tech, Hacienda San José s/n, Urcuquí, Ecuador
vanessa.hinojosa@yachaytech.edu.ec

In recent years, carbon nanotubes have generated a lot of interest in the nanotechnology field due to their extraordinary electronic and mechanical properties and as a reinforcement material.[1,2] They have been used to enhance the properties of a certain material. In the same way, clays formed by layers have been used widely due to their silicate layers, cation exchange capacity, and higher aspect ratios. It was found that composites made of Kaolinite (Kaol) present excellent thermal properties, flame retardant, barrier, and mechanical.[3] However, there is not much information about the spectroscopic and microscopic characterization of the clay, even less information about a composite made of Kaolinite and Carbon Nanotubes. It is of great interest to understand the behavior of interaction of those materials which gives information about their physical properties. In this work, it is presented a deep analysis of Raman characterization of a novel nanocomposite of multi-wall carbon nanotubes (MWCNT) and Ecuadorian kaolinite (Kaol). It was generated via sonication of Kaol in water and multiwall carbon nanotubes in isopropanol, and the nanocomposites were made varying the weight percentage of MWCNT in relation to Kaol (5, 1, 0.1, and 0.05% wt). Raman measurements reveal functionalization between both materials, with the highest functionalization in the lowest concentration of MWCNT. Scanning electron microscope (SEM) measurements were made to confirm Raman results which show MWCNT intercalating the Kaol structure.

References

[1] Price, G. J.; Nawaz, M.; Yasin, T.; Bibi, S. *Ultrasonics Sonochemistry* **2018**, *40*, 123–130.

[2] Andrews, R.; Jacques, D.; Qian, D.; Rantell, T. *Accounts of Chemical Research* **2002**, *35*, 1008–1017.

[3] Neto, J. M.; Kimura, S. P.; Vieira, M. G.; Neto, J. E.; Nascimento, N. R.; Lona, L. M. F. *Chemical Engineering Transactions* **2017**, *57*, 1453–1458.

Silver Nanostructures Morphology Tunned by Reducing and Capping Agent Involved in its Green Synthesis

Araceli Granja[1]
Floralba López[1], Nayely Pineda[2]
[1] *School of Chemical Science and Engineering Yachay Tech, Urcuquí, Ecuador*
[2] *Cimav Monterrey, Monterrey, Mexico*
lourdes.granja@yachaytech.edu.ec

A procedure for the synthesis of silver nanoparticles is presented in which their size and shape are controlled modulating nucleation and particle growth processes by means of suitable proportions of reducing and capping agents. Colloidal suspensions of nanoparticles were obtained whose absorption of light covers the spectrum from 400 nm to 700 nm, which correspond from spherical nanoparticles to nanoprisms, according to the literature.[1] In addition, we show the effectiveness of garlic extract, whose main component is Aliicine, and the cinnamon bark extract, whose main component is the cinnamaldehyde, as a reducing and capping agent in the process of nanoparticle synthesis. Depending on reducing/capping agent different shapes are obtained; by the use of garlic extracts result mainly spherical particles, while that a greater diversity of shape is obtained with the bark cinnamon. The stability of the colloidal dispersion extends for several months. Both, some bactericidal activity and an increase of the conductivity of pectin films with silver nanoparticles embedded in that polymer were evidenced, which imply future potential applications. Characterization of the silver nanoparticles was performed with UV spectroscopy, with scanning transmission spectroscopy (STEM), scattering electronic microscopy (SEM) and impedance technique.

Figure 13. UV-Vis Spectroscopy of Silver Nanoparticles

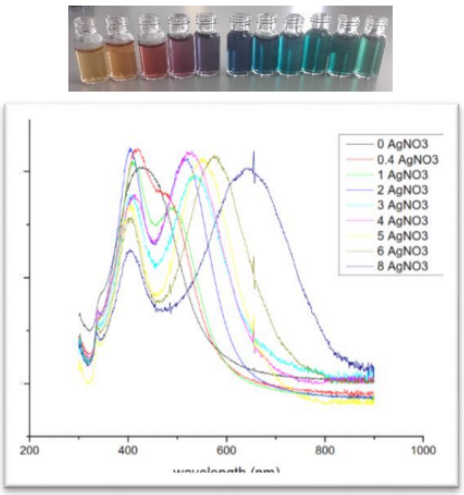

Figure 14. Spherical Silver Nanoparticles (u), Nanoprisms(d)

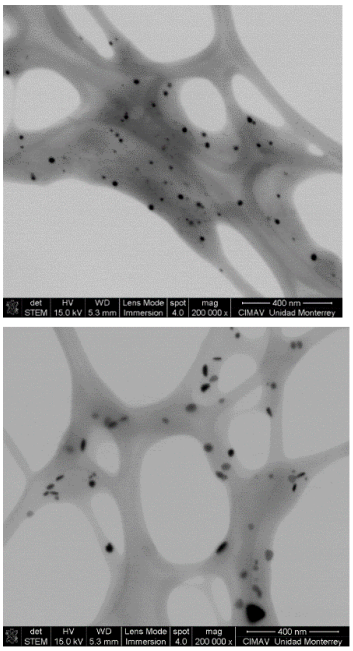

References

[1] ANKER, J. N.; HALL, W. P.; LYANDRES, O.; SHAH, N. C.; ZHAO, J.; DUYNE, R. P. V. *Nanoscience and Technology*; Co-Published with Macmillan Publishers Ltd, UK, 2009; pp 308–319.

First Principles Band Gap Engineering Of Graphene Quantum Dots

Cristina Mina
Miguel Ángel Suarez, Miguel Ojeda, and J. L. Cuevas
Yachay Tech University, School of Physical Science and Nanotechnology 100115, Urcuquí, Ecuador.
maria.mina@yachaytech.edu.ec

Nowadays, the nanomaterials based on graphite as graphene, nanotubes, fullerenes or quantum dots have been attracted much attention due to the possible applications on medicine, electronics or sensors.[1] Graphene quantum dots, which are nanometer-sized fragments of graphene where the electronic transport are confined in the three spatial dimensions, are very attractive for the tunable modification of the band gap by the quantum confinement effect[2] . In this wok, we performed a theoretical study of structural and band gap modification on graphene quantum dots with the diameter dependence. To perform this study 3 different GQD were modeled with diameters of 5.12 Å, 9.69 Å and 14.50 Å. The structural and electronic properties were calculated by DFT implemented in the SIESTA package.

Figure 15. Schematic representation of Graphene quantum dots.

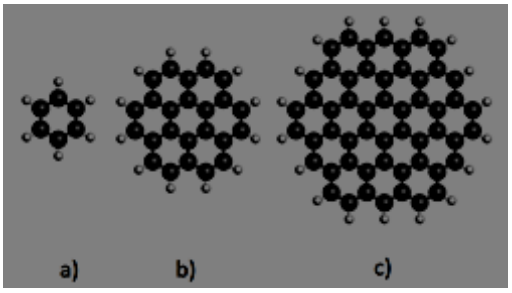

References

[1] Méndez Medrano, M. G.; Rosu, H. C.; Torres González, L. A. *Acta Universitaria* **2012**, *22*.

[2] Rodríguez González, C.; Kharissova, O. V. *Ingenierías* **2008**, *11*, 17–23.

[3] Bacon, M.; Bradley, S. J.; Nann, T. *Particle & Particle Systems Characterization* **2014**, *31*, 415–428.

Synthesis and characterization of bentonite clay with Multi-walled carbon nanotubes

Claudia Emilia Calderón Cordero
Julio Chacón, Yadira Vega,David Lajones, and Verónica Quilumba *Yachay Tech University, School of Physical Sciences and Nanotechnology, Urcuquí 100119, Ecuador*
claudia.calderon@yachaytech.edu.ec

Multi-walled carbon nanotubes (MWCNTs) have very particular structural properties that make them very interesting for technological applications.[1] On the other hand, bentonite clay is used in various fields, such as pharmaceutical ingredient, as waste material isolator, and as components for molecular engineering[2] because of its properties in morphology and chemical constitution.[2] In order to enhance the properties of bentonite clay, we intended to obtain an experimental nanocomposite of the mentioned clay with multi-walled carbon nanotubes. We used two different types of carbon nanotubes: MWCNTs purified with HCl,[3] and MWCNTs functionalized with COOH groups.[4] We made dispersions by sonication with each type of MWCNTs in distilled water adding sodium dodecyl sulfate (SDS) with a proportion of MWCNTs:SDS of 1:1.5,[5] and MWCNTs:water of 1mg:1ml. Then, we combined each of the dispersions with nanobentonite clay (≤25 μm) also by sonication, choosing different proportions of MWCNTs:bentonite (0.01:100, 0.05:100, 0.1:100, 0.5:100). The samples were characterized by X-ray diffraction (XRD) and by Scanning electron microscopy (SEM). The resulting diffraction patterns and SEM images show the changes of the bentonite clay when combining it with MWCNTs in different concentrations. The results suggest that carbon nanotubes were positioned in different parts of the surface of the clay, modifying the distances within its structure.

Figure 16. Computational simulation of bentonite clay slabs and multi-walled carbon nanotubes

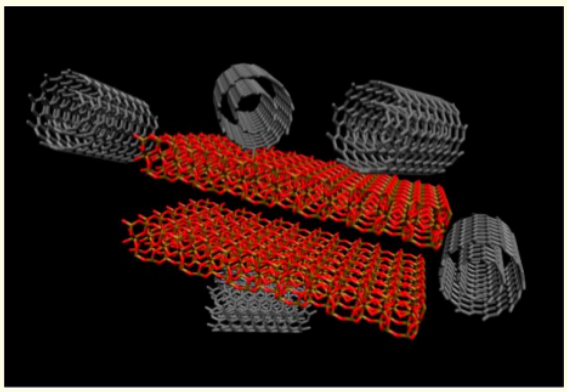

References

[1] Li, S.; Wang, Y.; Peng, S.; Zhang, L.; Al-Enizi, A. M.; Zhang, H.; Sun, X.; Zheng, G. *Advanced Energy Materials* **2015**, *6*, 1501661.

[2] Eisenhour, D. D.; Brown, R. K. *Elements* **2009**, *5*, 83–88.

[3] Datsyuk, V.; Kalyva, M.; Papagelis, K.; Parthenios, J.; Tasis, D.; Siokou, A.; Kallitsis, I.; Galiotis, C. *Carbon* **2008**, *46*, 833–840.

[4] Balasubramanian, K.; Burghard, M. *Journal of Materials Chemistry* **2008**, *18*, 3071.

[5] Yu, J.; Grossiord, N.; Koning, C. E.; Loos, J. *Carbon* **2007**, *45*, 618–623.

Rheological analysis of clay-carbon nanotubes composites as a potential application in drilling muds

V. Quilumba-Dutan
Luis Carrión, Christian Narvaez, and Julio C. Chacón-Torres.
Yachay Tech University, Urcuquí, Ecuador.

veronica.quilumba@yachaytech.edu.ec

Drilling fluids are vital components for oil, gas, water, and vapor extraction and production.[1] High temperature wells may cause difficulty in drilling operation.[2] Important properties such as viscosity of the drilling fluid may be affected by the thermal gradient inside the well. An excess of viscosity would make the fluid less pumpable, while on the other hand, if the fluid is very diluted, it will decrease the dragging capacity of the detritus.[3] The role of an optimal drilling fluid is to provide lubrication and cooling through its heat capacity and thermal conductivity, so that the drilling process is carried out without complications[4] .The addition of nanoparticles has proven to be a potential technique in the improvement of the rheological properties of drilling fluids due to their physico-chemical, electrical, thermal, and hydrodynamic properties.[5] In this study, a systematic rheological analysis from clay-nanocomposites mixed with multiwalled carbon nanotubes (MWCNT) in a matrix of bentonite was conducted. Several samples of clay-nanocomposites were prepared at different concentrations of MWCNT and water. The results reveal that the stability of viscosity of the clay-nanocomposites in concentrations of 0.01, 0.05 and 0.1 wt% slightly improves under high temperature conditions (120 ℃). These result will serve to contribute to the knowledge in drilling muds engineering for the Ecuadorian oil industry.

Figure 17. Evolution of viscosity at ambient temperature (23 ℃) and high temperature (120 ℃) evaluated at different concentrations of MWCNT (0.01, 0.05, and 0.1 wt%).

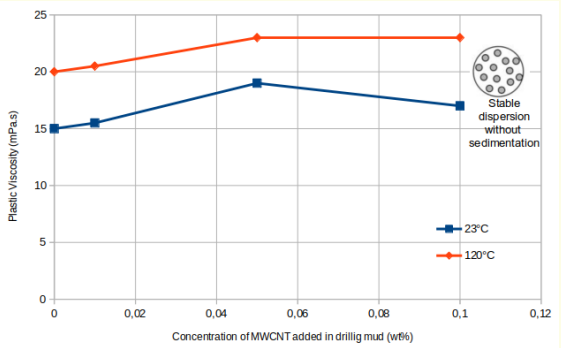

References

[1] et al., C. I. Manual de prácticas de laboratorio de fluidos de perforación de pozos. B.S. thesis, Universidad Central del Ecuador, 2018.

[2] Espinosa, S.; Stalin, C. Estudio y caracterización reológica de fluidos de perforación basados en agua y bentonita sódica natural. B.S. thesis, Universidad de las Fuerzas Armadas ESPE. Carrera de Ingeniería Mecánica., 2017.

[3] Ismail, A. R.; Rashid, N. M.; Jaafar, M. Z.; Sulaiman, W. R. W.; Buang, N. A. *Journal of Applied Sciences* **2014**, *14*, 1192.

[4] Villarroel Aguirre, L. C. Diseño de un fluido de perforación drill-in compuesto por carbonato de calcio para minimizar el daño en formaciones productoras en el campo Sacha. B.S. thesis, Quito: UCE., 2014.

[5] others„ et al. Preliminary test results of nano-based drilling fluids for oil and gas field application. SPE/IADC Drilling Conference and Exhibition. 2011.

Silver nanoprisms: an insight into the photochemical growth mechanism

Esteban D. Lasso
José A. Arcos-Pareja, Kevin Robalino, Alexis Debut, Sarah Briceño, and Julio Chacón
Yachay Tech University, School of Physical Sciences and Nanotechnology, 100119 Urcuquí, Ecuador.
esteban.lasso@yachaytech.edu.ec

On the last decade, anisotropic metallic nanoparticles became the subject of interest since open the possibility to use them in several fields like: labels for biochemical sensors, surface-enhanced spectroscopy, catalysts, optical switches, waveguides, light sources, and lithographic tools.[1,2] However, the chosen application of silver nanoplates depend strongly on their size and shape, meaning it is important to determine the factors that control the growing process. One of the synthesis methods is photo-induced growth, which has been considered the most controllable synthesis reaction, and thus providing a more suitable scenario to understand each step of the growing process.[3] In this photo-reaction, the use of trisodium citrate (TSC) as a capping agent is standard and well known to synthesize silver nanoplates.[4,5] However, a clear description of its influence in the growth mechanism process to shape spherical Ag nanoparticles into triangular nanoplates is not completely understood and remains a challenge for the precise synthesis of SNPs. In this work we describe a condensed mechanism for the photochemical growth of SNPs by taking into account the different variables involved in our experimental set-up, and compared them to the literature work of several groups. We explain how the pH of the solution and the capping agent (TSC) have a direct impact on the growth of these anisotropic particles while exposed to 440 nm, 520 nm, 650 nm and 3000 K radiation in a closed (Light Emission Diode) LEDs chamber. Additionally, we provide TEM images and a detailed UV-vis spectrum to describe and analyse the growth mechanism of the triangular Ag nanostructures.

Figure 18. Experimental set up.

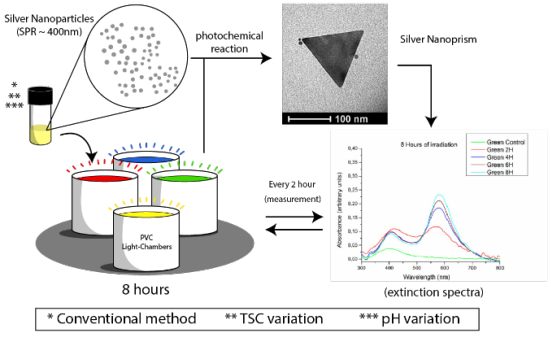

Figure 19. Photo reduction mechanism showing TSC reduction by effect of light and further growth of triangular plates caused by dipole and quadrupole resonances.

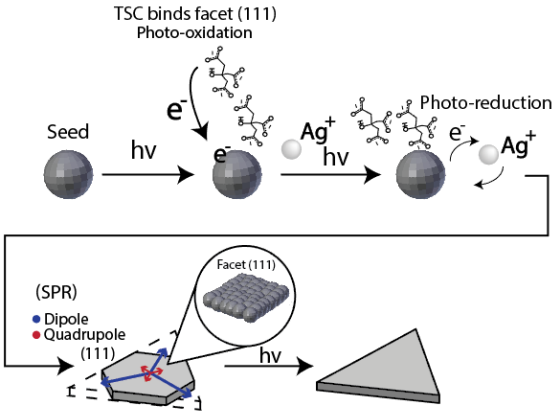

References

[1] Zhang, J.; Langille, M. R.; Mirkin, C. A. *Journal of the American Chemical Society* **2010**, *132*, 12502–12510.

[2] Zhang, Q.; Li, N.; Goebl, J.; Lu, Z.; Yin, Y. *Journal of the American Chemical Society* **2011**, *133*, 18931–18939.

[3] Saade, J.; de Araújo, C. B. *Materials Chemistry and Physics* **2014**, *148*, 1184–1193.

[4] Xue, C.; Métraux, G. S.; Millstone, J. E.; Mirkin, C. A. *Journal of the American Chemical Society* **2008**, *130*, 8337–8344.

[5] Xue, C.; Mirkin, C. *Angewandte Chemie International Edition* **2007**, *46*, 2036–2038.

Titanium dioxide/chitosan composite as photoconductant material

Lady Rios Andagoya[1]
Werner Brämer Escamilla, Gema González, and Mona Jani.
Yachay Tech. San Miguel de Urcuquí, Hacienda San José, Proyecto Yachay, Ecuador
lady.rios@yachaytech.edu.ec

In this work we present the study of photoconductance properties of Titanium dioxide in a matrix of Chitosan. The chitosan titanium composite solution was made via two different procedure, one in a 1wt.% aqueous acetic acid to promote the dissolution and the elimination of a bubble formation and the second in presence of polyvinyl alcohol.[1,2] For the photoconductance study a film of chitosan with titanium dioxide where dispose over various interdigitated electrode by spin-coating method. Three different interdigitated electrodes were constructed, first by sputtering second by chemical etching on bakelite sheet and third by soft masking using silver paint.[3,4] The measurement of photoconductance as function of the wavelength where performed using five different LED light source (397, 477, 522, 597, and 630 nm). The photoconductance as function of the wavelength of the titanium dioxide/chitosan composite layer is greater than the photoconductance response of a chitosan layer free from titanium dioxide, this behaviour is an advantage for new type of devices.

Figure 20. Process of developed titanium dioxide/chitosan composite photoconductivity films and photocontuctive measurement.

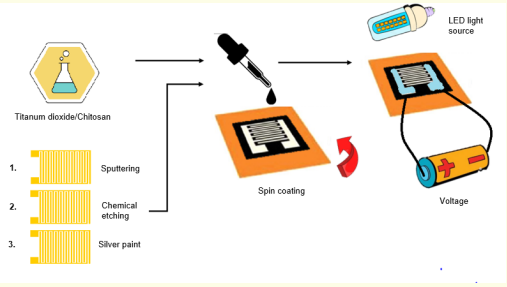

References

[1] Alagumuthu, G.; Kumar, T. A. *Int. J. Nanosci. Nanotechnol* **2013**, *4*, 105–111.

[2] Prokhorov, E.; Luna-Bárcenas, J. G.; González-Campos, J. B.; Sanchez, I. C. *Molecular Crystals and Liquid Crystals* **2011**, *536*, 24/[256]–32/[264].

[3] Kumar, N.; Sahatiya, P.; Dubey, P. *Procedia materials science* **2014**, *6*, 1976–1980.

[4] Chou, K.-S.; Lee, C.-H. *Advances in Materials Science and Engineering* **2014**, *2014*.

Structural and vibronic characterization of alkalimetal exfoliated GNRs dispersed in THF

Denise Andrade-Guevara
Julio C. Chacón-Torres, Claudia Kröckel, Frank Hauke, and Andreas Hirsch. *Yachay Tech University, School of Physical Sciences and Nanotechnology, Urcuquí, Ecuador*
denise.andrade@yachaytech.edu.ec

Graphene Nanoribbons (GNRs) are narrow strips of graphene that exhibit interesting electronic and magnetic properties based on its quantum confinement effects.[1] GNRs can be produced by a chemical evaporation deposition method (CVD), which for instance hampers the possibility to get individual GNRs that can be directly integrated to nanostructured electronic devices.[2] There exist bottom-up approaches along the synthesis of GNRs that has excel as an alternative to single individualization and integration of GNRs into quantum electronic devices.[3,4] These existing methods to obtain single monolayer GNRs or to individualize bundles of CVD grown GNRs, can be expensive and/or not suitable for a mass scale production.[4] In this work we have optimized a dispersion process for CVD grown GNRs in tetrahydrofuran (THF) vía a charge transfer mechanism method using sodium and potassium as electron donor species to individualize and get single dispersed graphene nanoribbons from bundles.

References

[1] Nakada, K.; Fujita, M.; Dresselhaus, G.; Dresselhaus, M. S. *Physical Review B* **1996**, *54*, 17954–17961.

[2] Zhang, T.; Wu, S.; Yang, R.; Zhang, G. *Frontiers of Physics* **2017**, *12*.

[3] Hawkins, P.; Begliarbekov, M.; Zivkovic, M.; Strauf, S.; Search, C. P. *The Journal of Physical Chemistry C* **2012**, *116*, 18382–18387.

[4] Celis, A.; Nair, M. N.; Taleb-Ibrahimi, A.; Conrad, E. H.; Berger, C.; de Heer, W. A.; Tejeda, A. *Journal of Physics D: Applied Physics* **2016**, *49*, 143001.

Figure 21. a) SEM micrograph of pristine GNRs produced by CDV at 5kV. b) Process of Intercalation and exfoliation of Sodium (i, ii) and potassium (iii, iv). c) Individualized GNR before Intercalation/Exfoliation process with Sodium and respective AFM profile figure.

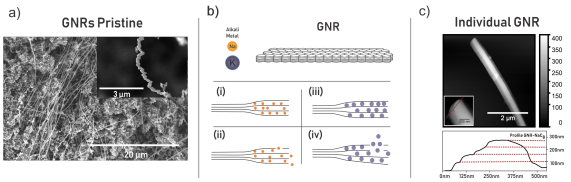

Figure 22. : (a) Optical microscope image of a GNR at 100x magnification obtained by dispersion of NaC_8 GNRIC. Top right corner: AFM image of the same GNR. (b) Optical microscope image of a GNR at 100x magnification obtained by dispersion of KC_{24} GNRIC. (Top right) AFM image of the same GNR. Raman spectrum (i), profile plot (ii) and AFM image (iii) of GNR obtained by dispersion of NaC_8 (c) and KC24 (d) GNRIC on THF after shake the sample.

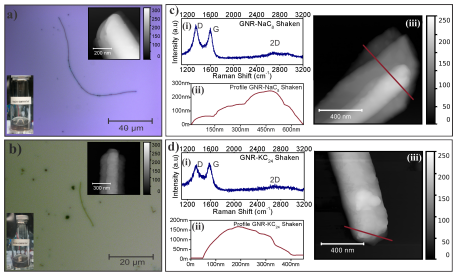

Figure 23. GNRs Intercalation/exfoliation process. (a)GNR Morphology at pristine stage. GNRs separate form each other during exfoliation (b) and get individualized (c). Few of them re-agglomerate forming thicker GNRs.

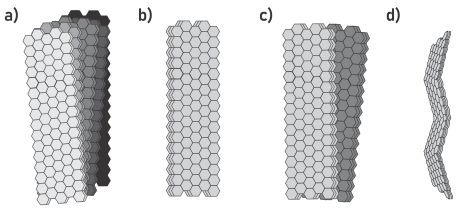

Unfolding the interaction between graphenechitosan by Raman Spectroscopy

Lorena Layana[1]
Charlotte Berrezueta, Andrés Guerrero, Sarah Briceño, Duncan Mowbray, and Julio C. Chacón-Torres
Yachay Tech University, School of Physical Sciences and Nanotechnology, Urcuquí 100119, Ecuador.
lorena.layana@yachaytech.edu.ec

Graphene is one the most studied materials due to its novel electronic, mechanical and optical properties[2] . It is known that graphene must be combined with other biocompatible molecules so that we can take advantage of the material in bioapplications[3] . Chitosan is a linear polysaccharide molecule composed of randomly distributed β–linked D-glucosamine and N-acetyl-D-glucosamine which results from the deacetylation of chitin.[4] Nanocomposites based in these two materials have been done for biotechnological purposes.[5] But, the graphene/chitosan matrix study have not been performed systematically, and the description of their interactions and functionalization has never been explained. We successfully developed an absolute graphene-chitosan composite though an ex-situ approach that can be of use to support for Au and Ag nanoparticles. In this study, we conducted an exhausting Raman spectroscopic analysis. We found new D modes present in our sample including a D_2 mode, which is an indicator of a sp_3 hybridization[6] formed within the graphene lattice. Computational calculations also support our findings in addition to atomic force microscopy, scanning electron microscopy and Fourier transform infrared spectroscopy analyses.

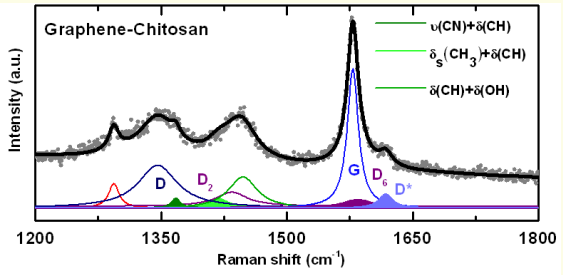

Figure 24. Raman spectrum of the Graphene-chitosan composite. The characteristic peaks of graphene (D, G line), chitosan[1] and the D_2 mode indicating the presence of a sp_3 hybridization are evident in this analysis.

Acknowledgments

Dear Park Systems,
I would like to start by saying how important the NSSY-2019 Galapagos is for me. As I mentioned in my motivation letter for the grant request, I'm convinced that one can learn more when sharing knowledge between people from all around the world. I am very grateful for your sponsorship, and I feel responsible for giving the best of me. Thank you for "striving everyday to live up to the innovative spirit of its beginnings" as you say.

References

[1] Zając, A.; Hanuza, J.; Wandas, M.; Dymińska, L. *Spectrochimica Acta Part A: Molecular and Biomolecular Spectroscopy* **2015**, *134*, 114–120.

[2] Jorio, A.; Dresselhaus, M.; Saito, R.; Dresselhaus, G. *ed: John Wiley & Sons*

[3] Liu, Y.; Wang, M.; Zhao, F.; Xu, Z.; Dong, S. *Biosensors and Bioelectronics* **2005**, *21*, 984–988.

[4] Kumar, M. N. R. *Reactive and functional polymers* **2000**, *46*, 1–27.

[5] Shan, C.; Yang, H.; Han, D.; Zhang, Q.; Ivaska, A.; Niu, L. *Biosensors and bioelectronics* **2010**, *25*, 1070–1074.

[6] Vecera, P.; Chacón-Torres, J. C.; Pichler, T.; Reich, S.; Soni, H. R.; Görling, A.; Edelthalhammer, K.; Peterlik, H.; Hauke, F.; Hirsch, A. *Nature communications* **2017**, *8*, 15192.

Pluronic P123 Copolymer as High Internal Phase Emulsion Stabilizer to Encapsulate Microalgae into Silica Monolith

Nadia Lopez-Pico
Si Amar Dahoumane, Thibault Terencio, and Alicia Sommer-Marquez
[1] *Universidad de Investigación y Tecnología Experimental Yachay Tech, Hacienda San Miguel de Urcuquí S/N, Urcuquí, Ecuador*
asommer@yachaytech.edu.ec

Pluronic P123 is a symmetric non-ionic triblock copolymer and it has different applications such as: emulsion stabilizer,[1] pharmaceutical ingredient,[2] biomedical materials,[3]template of mesoporous materials,[4] among others. The use of this polaxamer can also give place to the obtaining of hierarchical silica monoliths by using emulsion-polymer double template.[5] This method allows to synthesize, in one-pot process, silica monoliths with a high controlled macro and mesoporosity keeping also a high surface area when porosity is free, Figure 1. Several work has been done in the encapsulation of living plant cells, cyanobacterias or microalgae into different matrices.[6,7] However, some challenges in immobilization have to be taking into account, for example: maintaining a high metabolic activity over an extended period of time, maintaining gel surface sterility, designing optimal encapsulation protocols, understanding of cellular response to encapsulation, controlling of gelation and pore structure, among others. In one hand, we will control the excessive growth of algae caused by eutrophication, which has become a problem in aquatic environment and, in another, to keep their vital function and utilize them as a CO_2 adsorbers. Due to P123 properties and biocompatibility, it was chosen to perform the encapsulation of microalgae into silica monoliths. An innovative way to encapsulate microalgae within silica monoliths containing P123 for both, emulsion stabilization a

Figure 25. SEM microscopy and BET area of Si-monolith with free porosity

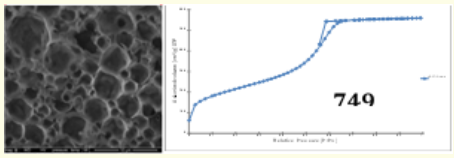

Figure 26. Encapsulation of Algae by HIPE

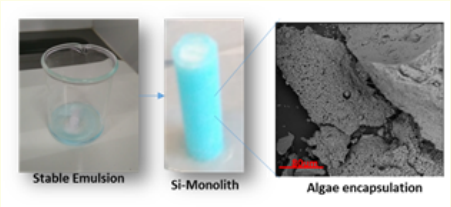

References

[1] Barnes, T. J.; Prestidge, C. A. *Langmuir* **2000**, *16*, 4116–4121.

[2] Yang, L.; Alexandridis, P. *Current Opinion in Colloid & Interface Science* **2000**, *5*, 132–143.

[3] Ahmed, F.; Alexandridis, P.; Shankaran, H.; Neelamegham, S. *Thrombosis and Haemostasis* **2001**, *86*, 1532–1539.

[4] Zhao, D. *Science* **1998**, *279*, 548–552.

[5] Zhang, Z.; Han, M. *Journal of Materials Chemistry* **2003**, *13*, 641–643.

[6] Meunier, C. F.; Rooke, J. C.; Léonard, A.; Cutsem, P. V.; Su, B.-L. *J. Mater. Chem.* **2010**, *20*, 929–936.

[7] Pressi, G.; Toso, R. D.; Monte, R. D.; Carturan, G. *Journal of Sol-Gel Science and Technology* **2003**, *26*, 1189–1193.

Wednesday

Nanomaterials anomaterials in heterogeneous photocatalysis: photocatalysis from fundamentals to applications

Adriana Zaleska-Medynska

University of Gdansk, Faculty of Chemistry, Department of Environmental Technology, Technology Wita Stwosza 63, 80-308 Gdansk, Poland

adriana.zaleska@ug.edu.pl

Photocatalytic reactions over semiconductor nanoparticles have been proposed as an environmental friendly and promising approach to remove pollutants from gas and liquid phase, to generate hydrogen *via* water splitting process, as well as, to transform low value chemicals into higher value using solar irradiation. Efficiency of the photocatalytic process is affected by: *(i)* type of semiconductor material (e.g. band gap structure); *(ii)* (morphology and surface face properties of semiconductor nanoparticles; *(iii)* (irradiation range and intensity; *(iv)*) type and concentration of substrates; and *(v)*) photoreactor geometry.[1] Following topics will be presented during the lecture:

1. Mechanism of the heterogeneous photocatalysis catalysis and semiconductor requirements for photocatalytic reactions (Figure 27-29);
2. Preparation of selected semiconductor materials in the form of quantum dots, thin films and three dimensional nanostructures;
3. Application of heterogeneous photocatalysis in degradation of pollutants in the gas and liquid phase, water and air disinfection, self- self cleaning surfaces, water splitting , biomass bioma conversion, artificial photosynthesis and green synthesis.

Figure 27. Formation of active oxygen species at the semiconductor nanoparticle surface after light absorption: (i) initiation of an oxidative pathways of electron donors by valence band (VB) holes (h^+); (ii) initiation of a reductive pathway of electron acceptors (i.e. O_2) by conduction band (CB) electrons

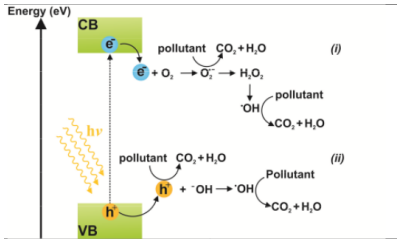

Figure 28. Mechanism of photocatalytic water splitting for hydrogen generation over semiconductor nanoparticles

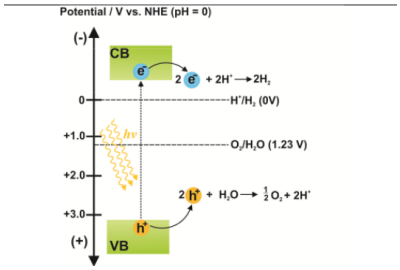

Figure 29. Mechanism of photocatalytic reduction of CO_2 with H_2O on a semiconductors photocatalysts by suitable redox co-catalyst

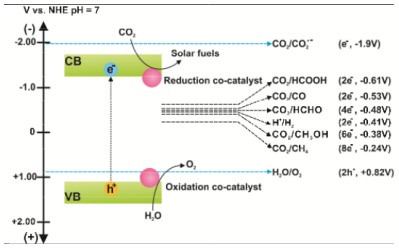

References

[1] Fattakhova-Rohlfing, D.; Zaleska, A.; Bein, T. *Chemical reviews* **2014**, *114*, 9487–9558.

[2] Zaleska-Medynska, A. *Metal Oxide-based Photocatalysis: Fundamentals and Prospects for Application*; Elsevier, 2018.

Tailoring Magnetic SiO_2-$Mn_{1-x}Co_xFe_2O_4$ Nanocomposites Decorated with Au@Fe_3O_4 Nanoparticles for Hyperthermia

Sarah Briceño[1,2]
Viviana Daboin [1], Jorge Suarez[1],Olgi Alcalá [1], Lila Carrizales [1], Pedro Silva[1], and Gema González [1,2]
[1] *Instituto Venezolano de Investigaciones Científicas (IVIC), Apartado 20632, Caracas 1020-A, Venezuela.*
[2] *Yachay Tech University, School of Physical Sciences and Nanotechnology, 100119-Urcuquí, Ecuador.*
sbricenio@yachaytech.edu.ec

Herein, we present the design of magnetic mixed manganese-cobalt ferrite nanoparticles $Mn_{1-x}Co_xFe_2O_4$ coated with silica (SiO_2) anddecorated with Au@Fe_3O_4 nanoparticles as magnetic fluid hyperthermia heat mediators. $Mn_{1-x}Co_xFe_2O_4$ NPs were synthesized using the thermal decomposition method, subsequently coated with SiO_2 following the Stober method and decorated with Au@Fe_3O_4 nanoparticles. Structural characterization was carried out applying X-ray diffraction (XRD), infrared spectroscopy (FTIR), and transmission electron microscopy (TEM). Magnetic properties as a function of the Mn^{+2} content were studied using a vibrating sample magnetometer (VSM) at room temperature. Hyperthermia investigations were performed at 454 ± 20 kHz with a magnetic field amplitude of up to 5:5 mT. The specific absorption rate (SAR) values of the nanocomposites were found to have increased with the Au@Fe_3O_4 decoration in water. The advantage of the designed nanocomposite system lies in the fact that versatile combinations of magnetic NPs, SiO_2, and Au@Fe_3O_4 can modify the magnetic properties to optimize the Specific Absorption Rate (SAR).

Figure 30. TEM images of the undecorated (Right) and decorated (Left) nanocomposites and average particle size distribution for different Mn^{+2} content: (a) $CoFe_2O_4$ (x = 0), (b) $Mn_{0.25}Co_{0.75}$ Fe_2O_4 (x = 0.25), (c) $Mn_{0.5}Co_{0.5}Fe_2O_4$ (x = 0.50), (d) $Mn_{0.75}Co_{0.25}Fe_2O_4$ (x = 0.75) and (e) $MnFe_2O_4$ (x = 1).

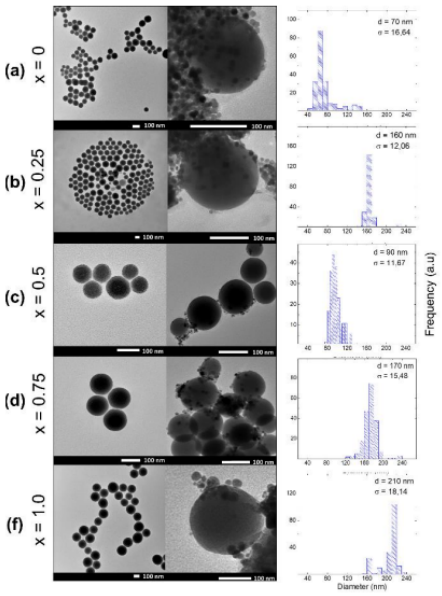

References

[1] Daboin, V.; Briceño, S.; Suárez, J.; Carrizales-Silva, L.; Alcalá, O.; Silva, P.; Gonzalez, G. *Journal of Magnetism and Magnetic Materials* **2019**, *479*, 91–98.

Unprecedented Record on Substitutional B-Doped Single-Walled Carbon Nanotubes

Carlos Reinoso[1,2]
Claudia Berkmann[1], Lei Shi[1,3], Alexis Debut [4], Kazuhiro Yanagi[5], Thomas Pichler[2], and Paola Ayala[2]
[1] *Yachay Tech University, School of Physical Sciences and Nanotechnology Urcuquí Ecuador*
[2] *University of Vienna, Faculty of Physics. Boltzmanngasse 5, A-1090 Vienna, Austria*
[3] *School of Materials Science & Engineering, Sun Yat-sen University, 510275 Guangzhou, Guangdong, P. R. China*
[4] *Centro de Nanociencia y Nanotecnologa, Universidad de las Fuerzas Armadas–ESPE, P.O. Box 171102,Sangolqui, Ecuador*
[5] *Department of Physics, Tokyo Metropolitan University, Hachioji, 192-0397 Tokyo, Japan*
creinoso@yachaytech.edu.ec

Single-walled carbon nanotubes doped with Boron have been synthesized from sodium tetraphenyl borate at the highest percentage reported for a raw material. However, several byproducts including carbonaceous impurities can still contain boron and therefore show diverse brands of competing bonding environments. To solve this controversy, which has constantly interfered a conclusive insight to the existing bonding environments in materials alike, we have engaged a purification method, which leaves ~ 7 % at. of B atoms of the total sample composition almost exclusively in the sp_2 electronic configuration. This represent on one hand a substitutional B-doping record, and, on the other hand, from X-ray photoelectron spectroscopy an unambiguously identification of the competing bonding environments. The doping level finded in the purified structures is about an order of magnitude larger than in other B-doped single-walled tubes even without purification, this represents a closer step to the controlled applicability of this functionalized material.

Figure 31. Boron-incorporation profile reaching ~ 7% on SWNT samples after the use of the purification procedures keeping a sp_2 electronic onfiguration.

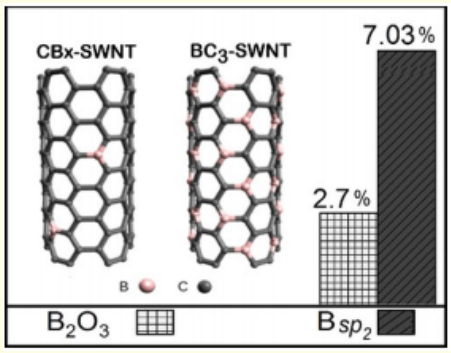

References

[1] Reinoso, C.; Berkmann, C.; Shi, L.; Debut, A.; Yanagi, K.; Pichler, T.; Ayala, P. *ACS Omega* **2019**, *4*, 1941–1946.

[2] Reinoso, C.; Shi, L.; Domanov, O.; Rohringer, P.; Pichler, T.; Ayala, P. *Carbon* **2018**, *140*, 259–264.

[3] Ruiz-Soria, G.; Susi, T.; Sauer, M.; Yanagi, K.; Pichler, T.; Ayala, P. *Carbon* **2015**, *81*, 91–95.

Hardness and structural properties of multiwall carbon nanotubes and aluminum-based composites

Eric Plaza[1,2]
M. Villalonga[1], J. Arévalo[1,3], R. Atencio[1,2], L. Corredor [4], R. Morales[3],M. Ramos [2], and A. Briceño [2]
[1]*Escuela Superior Politecnica del Litoral. (ESPOL) Guayaquil, Ecuador.*
[2] *Venezuelan Institute for Scientific Research (IVIC), Caracas, Venezuela.*
[3]*Zulian Technological Research Institute (INZIT), Maracaibo, Venezuela.*
[4] *School of Physical Sciences and Nanotechnology, Yachay Tech University, 100119 Urcuquí, Ecuador.*
ericvpp@gmail.com evplaza@espol.edu.ec

Powder Metallurgy was used in the preparation of the reinforced aluminium composite material with multiwall carbon nanotubes (MWCNT). MWCNT were synthesized by Chemical Vapor Deposition (CVD), using C2H2 as precursor gas, Ar as a carrier gas and Fe-Co/CaCO3 as a catalyst. The aluminium powder was mixed with CNT in different ratios from 0% to 2% and different times stages in the mixing process in a planetary mill (3 min and 1 h). The powders compounds were doubled hot-pressed and sintered. Compounds were analysed using a Field Emission Scanning Electron Microscope, X-ray powder diffraction, Thermogravimetric analysis, and Vickers Hardness. Results have shown a hardness-increasing for the compound up from ~14 % to 27.99 %. A total of 80 samples were examined to evaluate the effect of the CNT in the hardness compounds, we take the standard deviation of hardness as a measure of dispersion of CNTs.

Functionalization of Nanostructures: Chemical modification and advanced analysis

Carla Bittencourt
University of Mons, Place du Parc, 22, Mons, Belgium
carla.bittencourt@umons.ac.be

The concept of adding a 'selected' functionality to a material surface appeared nearly 2.6 million years ago, the surface of stones, wood and bones were designed into hammers, harpoons, needles, spears, etc. Through the human history timeline, strategies to add functionalities to a material via surface modification evolved from simple morphology changes (Stone Age) to surface chemical modification (Modern Age). The combination of different methods of surface modification can extend the range of optimal applications.

We will discuss different surface chemical functionalization strategies focusing on low- kinetic energy ion irradiation. A common misconception is that the irradiation with ions has exclusively detrimental effects on the properties of target materials.[1] Graphene based nanostructures will be used as model surfaces for chemical functionalization studies. Differences on ion irradiation of suspended and supported nanostructures will be presented. Concepts of implantation, functionalization and defect creation will be discussed.

Parallel to novel functionalization methods, new characterization tools have been developed. During this talk we will focus on characterization of functionalized nanostructres using two spectromicroscopy tools: the scanning photoelectron miscroscopy (SPEM)[2] installed at ELETTRA-Trieste and the transmission X-ray miscroscopy combined with near Near Edge X-ray Absorption Fine Structure[3,4] (TXM-NEXAFS) installed at BESSY II – Berlin. Both techniques allow the analysis of selected regions at the nanoscale.

Figure 32. Examples of surface functionalization (left) and characterization (right)

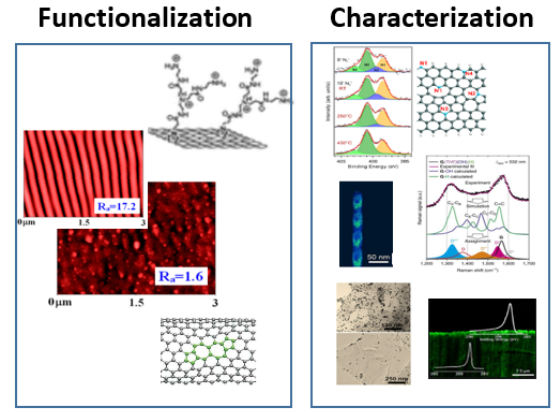

References

[1] Krasheninnikov, A.; Nordlund, K. *Journal of applied physics* **2010**, *107*, 3.

[2] others„ et al. *physica status solidi (a)* **2018**, *215*, 1800308.

[3] Guttmann, P.; Bittencourt, C. *Beilstein journal of nanotechnology* **2015**, *6*, 595–604.

[4] Guttmann, P.; Bittencourt, C.; Rehbein, S.; Umek, P.; Ke, X.; Van Tendeloo, G.; Ewels, C. P.; Schneider, G. *Nature Photonics* **2012**, *6*, 25.

One step synthesis of Fe/Ti oxide nanostructures from Ecuadorian black sands

Víctor Guerrero[1]
Emilio Pardo [2], Bojan A. Marinkovic[3], and Patricia I. Pontón [1]

[1] *Department of Materials, Escuela Politécnica Nacional, Ladrón de Guevara E11-253, Quito, Ecuador*
[2] *Molecular Science Institute, Coordination Chemistry Group, University of Valencia, Polígono la comas/n, Paterna, Spain*
[3] *Department of Chemical and Materials Engineering, Pontifical Catholic University of Rio de Janeiro (PUC-Rio), CP 38008, 22453-900, Rio de Janeiro, RJ, Brazil*
victor.guerrero@epn.edu.ec

TiO_2 based nanostructures have attracted special attention due to their photocatalytic activity, ion exchange capacity and high specific surface area. These are key properties in applications such as energy storage and pollutants photodegradation.[1] However, these nanostructures can only absorb radiation in the UV region. This drawback might be overcome through their doping with metal ions (i.e. Fe) in order to enhance their efficiency of absorbing visible radiation. The conventional route for the synthesis of Fe/Ti oxide nanostructures, generally involves expensive reactants and complex procedures. Another promising approach, but even less explored, is based on the alkaline hydrothermal treatment (AHT) of low cost and unrefined natural precursors, such as ilmenite beach sands, that contain Fe and Ti in their crystal structures[2] Large reserves of this mineral are located in the northern coast of Ecuador (Mompiche- Esmeraldas). These black sands are fairly attractive from the point of view of their phase composition that does not only comprise ilmenite (45-56%), but also hematite and magnetite, ranging from, 25-37 % and 10-17%, respectively. Since Ecuadorian black sands exhibit a high Fe content, TiO_2 – based nanostructures doped with Fe can be synthesized during AHT, while the excess of Fe could re-precipitate as nanohematite and/or nanomagnetite. This opens a framework to prepare hybrid nanostructures in just one step soft-chemistry synthesis. These nanostructures would also exhibit magnetic properties, which are of paramount importance in industrial processes that imply their removal from aqueous media. Hence, the aim of this work is to synthesize Fe/Ti oxide hybrid nanostructures in a single step, from unrefined Ecuadorian black sands. These sands were ball milled and fed into a Teflon reactor to conduct the AHT, using a 10 M NaOH aqueous solution under vigorous stirring. The reaction time was defined as 70 h and temperatures between 110 °C and 190 °C were selected to evaluate the effect of this variable on the phase composition of the as- synthesized nanostructures. X-ray powder diffraction (XRPD) and scanning electron microscopy with energy dispersive spectroscopy (SEM-EDS) analyses were performed to identify the crystalline phases and elemental composition of the as-prepared nanostructures, respectively. Their morphology was evaluated by transmission electron microscopy (TEM), while their specific surface area was measured by N_2 adsorption using Brunauer–Emmett–Teller (BET) method. This research shows an inexpensive approach for the synthesis of Fe/Ti oxide hybrid nanostructures and the importance of further studies to determine the photocatalytic and magnetic properties of these nanostructures.

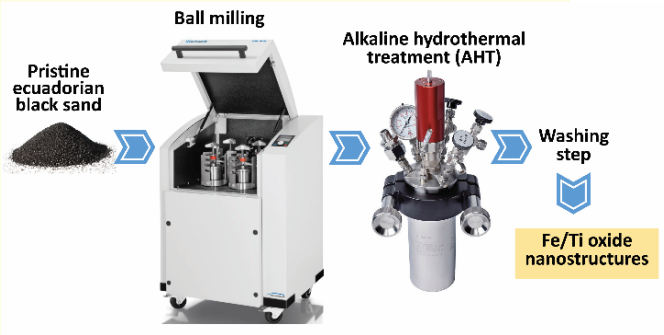

Figure 33. Procedure for the synthesis of Fe/Ti oxide nanostructures by alkaline hydrothermal treatment (AHT) from Ecuadorian black sands.

References

[1] Gázquez, M. J.; Bolívar, J. P.; Garcia-Tenorio, R.; Vaca, F. *Materials Sciences and Applications* **2014**, *5*, 441.

[2] Jardim, P. M.; Mancic, L.; Marinkovic, B. A.; Milosevic, O.; Rizzo, F. *Central European Journal of Chemistry* **2011**, *9*, 415–421.

Thursday

Theory and computation in nanoscience

Risto Nieminen
Department of Applied Physics, Aalto University, Box 11000, 00076 AALTO, Finland
risto.nieminen@aalto.fi

The number of possible atomic-scale combinations and configurations in nanostructures is astronomical. To facilitate the search for materials and structures with desired properties, powerful theoretical and computational multiscale methods are needed. This talk surveys the current state of the art in such methods. In particular, quantum-scale electronic-structure methods [1] based on density-functional theory and its extensions, applicable for both ground-state properties and excitations (spectroscopy), are discussed.
The talk also explores the application of machine-learning methods to the rapidly growing databases of materials properties.
As specific application examples, the cases of quantized conductivity and plasmonic response in ultrathin atomic wires as well as the search for novel 2D materials are presented.

Figure 34. The exponential growth of computing power enables multiscale materials modelling for computational materials design and discovery.

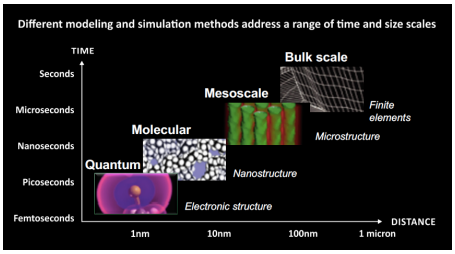

Figure 35. Big data and machine learning meet physics and chemistry.

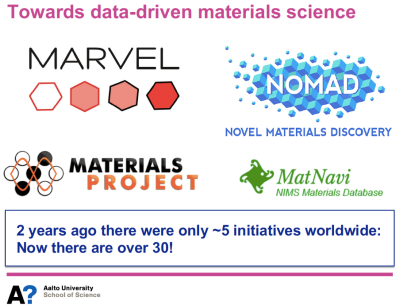

References

[1] Martin, R. M. *Electronic Structure*; Cambridge University Press, 2004.

Bonding with Parallel Spins in Lithium clusters

Luis Rincón[1]

[1] *Universidad San Francisco de Quito (USFQ), Grupo de Química Computacional y Teórica (QCT-USFQ), Departamento de Ingeniería Química, Colegio Politécnico de Ciencias e Ingeniería, Diego de Robles y Via Interoceanica, Quito 17-1200-841, Ecuador*

lrincon@usfq.edu.ec

Electron pairing constitutes the principal bonding mechanism in almost any molecule, in contrast, triplet pairs bonds is an elusive bonding mechanism due to the Pauli repulsion. Nevertheless, nowadays it is accepted that high-spin clusters of univalent atoms (Li, Na, Cu, Ag, Au), even without having a single electron pair in the valence shell, should be bonded.[1,2] This bonding mechanism was called no-pair ferromagnetic bond. Because real no-pair ferromagnetic bonds are typically investigated using modern DFT calculations, it seems important to check the accuracy of common exchange-correlation functional in these high-spin unusual situations. In this work, we will explore the performance of 20 functionals, compared to CCSD(T), for clusters from dimer to decamer. The tested functional involved pure-Local, pure-GGA, meta-GGA, hybrids and double-hybrids. In all cases, DFT functionals show very small distances, for example, in the best hybrid functionals a shortening of 20-30 % in the bond distance compared with CCSD(T) is observed. To understand this behavior, we study the electron localization due to the influence of the Coulomb hole using the information content of the conditional pair density[3]

References

[1] Danovich, D.; Shaik, S. *Accounts of chemical research* **2013**, *47*, 417–426.

[2] Danovich, D.; Shaik, S. *Annual review of physical chemistry* **2016**, *67*, 419–439.

[3] Urbina, A. S.; Torres, F. J.; Rincon, L. *The Journal of chemical physics* **2016**, *144*, 244104.

Ab initio study of 2D plasmon enhancement in alkali intercalated graphene on metallic substrates

Vito Despoja[1]
Leonardo Marušić [2]

[1] *Institute of Physics, Zagreb*
[2] *Maritime Department, University of Zada*
vito@phy.hr

Alkali metal (AM) atoms, (e.g. in LiC_2 or CsC_8) donate electrons to the graphene π band causing the appearance of the strong Dirac plasmon (DP) in the EEL spectra. At the same time, the AM σ band remains partially filled and supports another 2D plasmon, which hybridizes with the Dirac plasmon causing appearance of the weak linearly dispersive plasmon, known as the acoustic plasmon (AP).[1,2] We present the results of a theoretical simulation of alkali atoms intercalated between the graphene and a metallic substrate (e.g. Ir(111) or Al(111)) and forming a periodic superlattice, which causes a huge enhancement of DP and AP. Moreover the AP intensity and Fermi velocity strongly depend on graphene/substrate separations. This enhancement mechanism, in addition to its very interesting fundamental aspect, suggests many possibilities for plasmonic applications. The theoretical simulation is performed using a state of the art DFT (ground state) + RPA (excited state) technique, adapted for the study of the dielectric properties in large multilayer heterostructures, which completely exclude inter-supercell Coulomb interaction.

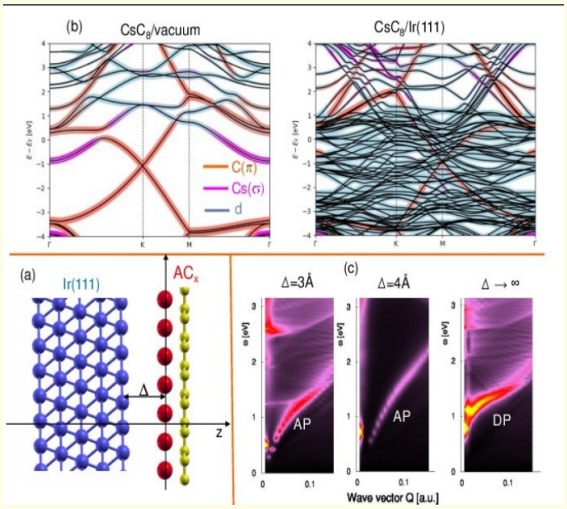

Figure 36. (a) Geometry of the composite system Ir(111)/CsC_8 . (b) Band structure in CsC_8 (left) and in Ir(111)/CsC_8 composites. (c) Surface loss function (EELF) in Ir(111)/CsC_8 composite for various Ir(111) and CsC_8 separations Δ. Equlibrium Ir(111) and CsC_8 separation is $\Delta = 3\text{Å}$.

References

[1] Marušić, L.; Despoja, V. *Physical Review B* **2017**, *95*, 201408.

[2] Despoja, V.; Marušić, L. *Physical Review B* **2018**, *97*, 205426.

Two-photon Spectroscopy using Intense Entangled Photon Beams

Jiří Svozilík[1,2]
Jan Peřina Jr.[2], and Roberto de J. León-Montiel[3]
[1] *Universidad Yachay Tech, Urcuquí, Ecuador*
[2] *Joint Laboratory of Optics of Palacký University and Institute of Physics of AS CR, Olomouc, Czech Republic*
[3] *Instituto de Ciencias Nucleares, Universidad Nacional Autónoma de México, Ciudad de México, México*
jsvozilik @ yachaytech.edu.ec

Time-resolved spectroscopic methods, such as the pump-probe spectroscopy, allow to measure the excitation dynamics inside examined materials. In recent years, a large attention has been devoted to optically-based methods using the quantum features of light permitting to increase the detection resolution and also efficiently increase the interaction of samples with a probing light.[1] Among various approaches, the virtual state spectroscopy[2,3] offers the possibility of resolving intermediate levels in the process of two-photon absorption. Usual approach based on the solution of the Schrödinger equation describes an ideal case of only one photon pair interacting with the considered sample. This requires to maintain a low photon flux. Recent advances in both theoretical and experimental domains in the generation of intense entangled photon beams (twin beams) in the nonlinear process of spontaneous parametric down-conversion (SPDC)[4] enable to boost the atom-light interaction meanwhile quantum features of light persist. For that reason, we focus our study on effects occurring in the scenario when many (entangled) photons interact with the sample.[5,6] However, this implies the existence of contributions in the detected signal originating also from non-entangled correlations between participating photons. Additionally, we put our attention also to spectral properties of such intense beams with respect to the pump power and changes in detected spectra if photon fluxes are raised above a certain level. For our theoretical study, we considered a simple atom with transitions between the ground state |g⟩, three intermediate states |k⟩, state is chosen such that $E_f - E_g = hc/\lambda_{p0}$, where λ_{p0} nm is the central wavelength of the pump pulse with time duration τ_p and power P_p, that interacts with a nonlinear crystal of length L. Photon pairs are generated in the SPDC process in a nonlinear crystal. Between generated photons a time-delay τ is introduced. Information about intermediate transitions is then obtained by monitoring the two-photon absorption rate as a function of τ asas shown in the Figure 52(a). In the Figure 52(b), changes of the detected absorption spectrum with an increasing photon pair number N_s are presented.

Figure 37. Sketch of the experimental setup (a) and the resolved energy spectrum as depends on the pump power (b).

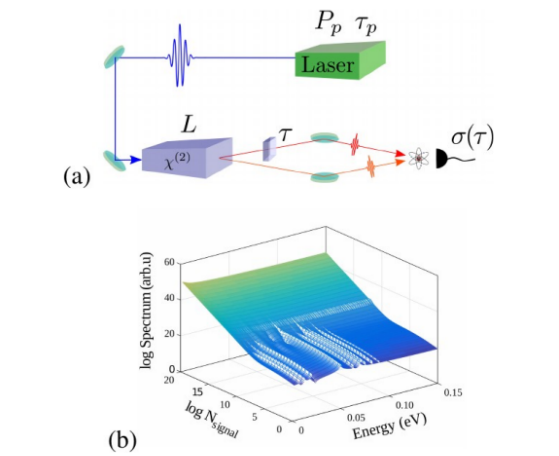

References

[1] Dorfman, K. E.; Schlawin, F.; Mukamel, S. *Reviews of Modern Physics* **2016**, *88*, 045008.

[2] Saleh, B. E.; Jost, B. M.; Fei, H.-B.; Teich, M. C. *Physical review letters* **1998**, *80*, 3483.

[3] de J León-Montiel, R.; Svozilik, J.; Salazar-Serrano, L.; Torres, J. P. *New Journal of Physics* **2013**, *15*, 053023.

[4] Machulka, R.; Haderka, O.; Peřina, J.; Lamperti, M.; Allevi, A.; Bondani, M. *Optics express* **2014**, *22*, 13374–13379.

[5] Svozilík, J.; Peřina, J.; León-Montiel, R. d. J. *Chemical Physics* **2018**, *510*, 54–59.

[6] Svozilík, J.; Peřina, J.; León-Montiel, R. d. J. *JOSA B* **2018**, *35*, 460–467.

Driven electronic transport in semi-Dirac materials

Alexander López[1]
[1] *ESPOL, Guayaquil,Ecuador*
tula1971@gmail.com

We present a model for the transport properties of a semi-Dirac material subject to ac driving. Exploring the quasi-energy spectrum, we find that certain directions in k-space remain insensitive to the modulation effects and use a low-energy effective Hamiltonian to show that by properly tuning the driving strength, pseudospin polarization inversion can be enhanced on demand by properly tuning the system parameters and establish the most appropriate conditions for an actual experimental realization of quantized conductance.

Proximity-induced spin-orbit effects in graphene on Au

Mayra Peralta
Alejandro López, Luis Colmenárez, Francisco Mireles, and Ernesto Medina
Yachay Tech University, School of Physical Sciences and Nanotechnology, 100115 Urcuquí, Ecuador
mperalta@yachaytech.edu.ec

We introduce a p_z-d coupling model Hamiltonian for the π-graphene/Au bands that predicts a rather large intrinsic spin-orbit (SO) coupling as is being reported in recent experiments and DFT studies.[1,2] Working within the analytical Slater-Koster tight-binding approach we were able to identify the overlapping orbitals of relevance in the enhancement of the SO coupling for both the sublattice symmetric (BC) and the ATOP (AC) stacking configurations. Our model effective Hamiltonian reproduces quite well the experimental spectrum for two registries, and in addition, it shows that the hollow site configuration (BC), in which the A/B sites remain symmetric, yields the larger increase of the SO coupling. We also explore the Audiluted case keeping the BC configuration and show that it renders the preservation of the SO gap with a similar SO interaction enhancement as the undiluted case but with a smaller graphene-gold distance.[3]

Figure 38. (a) Top: 3D vision of a cell in the BC stacking configuration of graphene on Au. Bottom: BC stacking configuration (b) Low energy dispersion for the BC stacking graphene-gold system. (c) Low energy dispersion for the BC system of diluted gold on graphene. (d) Graphene on a diluted gold surface. The dashed diamond delimits the unitary supercell formed by a gold atom and eight graphene carbons

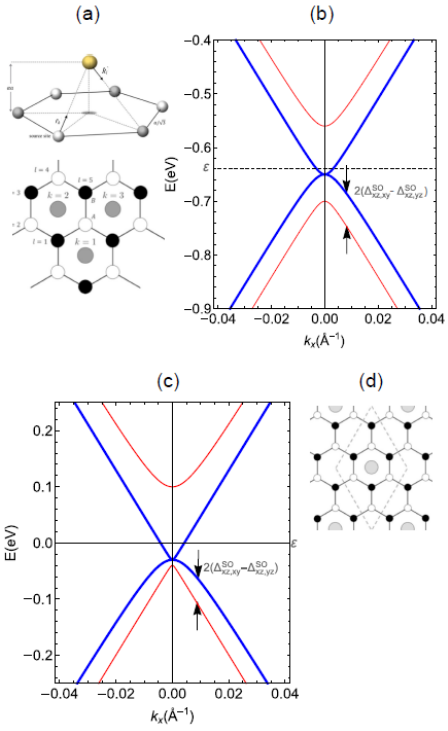

References

[1] Marchenko, D.; Varykhalov, A.; Scholz, M.; Bihlmayer, G.; Rashba, E.; Rybkin, A.; Shikin, A.; Rader, O. *Nature Communications* **2012**, *3*.

[2] Krivenkov, M.; Golias, E.; Marchenko, D.; Sánchez-Barriga, J.; Bihlmayer, G.; Rader, O.; Varykhalov, A. *2D Materials* **2017**, *4*, 035010.

[3] López, A.; Colmenárez, L.; Peralta, M.; Mireles, F.; Medina, E. *Phys. Rev. B* **2019**, *99*, 085411.

Electron transport simulations of multi-terminal nanoscale devices

Thomas Frederiksen[1,2]

[1] *Donostia International Physics Center (DIPC), Paseo Manuel de Lardizabal 4, E-20018 Donostia-San Sebastián, Spain*

[2] *IKERBASQUE, Basque Foundation for Science, E-48013, Bilbao, Spain*

thomas_ frederiksen@ehu.eus

In this talk I will describe some recent progress in the use of density functional theory (DFT) in combination with nonequilibrium Green's functions (NEGF) to describe the electronic structure of open quantum systems and to compute electron transport characteristics of nanoscale systems connected to multiple electrodes.[2] Examples include a proposal that two overlapping graphene nanoribbons (GNRs) under suitable conditions can operate as an electron beam splitter[1] (Fig. 39) and studies of scanning tunneling probe geometries to measure electron transport in nanoporous graphene[3] and through the anisotropic surface states of germanium (001).[4]

Support from the Spanish Ministerio de Economía y Competitividad (MINECO) (FIS2017-83780-P) is gratefully acknowledged.

Figure 39. Electron beam splitting in devices of two crossed GNRs separated by a van der Waalsdistance of ~ 3.3 Å. **(a)** In a 90 degree crossing, electrons injected from electrode 1 are mostly transmitted to electrode 2. **(b)** In a 60 degree intersection, the incoming electron from electrode 1 is split with a near 50-50 probability into the outgoing electrodes 2 and 4, in analogy with an optical beam splitter. Adapted from Ref.[1]

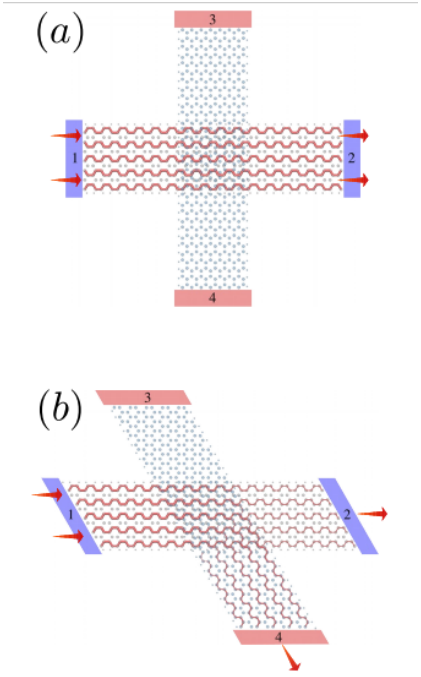

References

[1] Brandimarte, P.; Engelund, M.; Papior, N.; Garcia-Lekue, A.; Frederiksen, T.; Sánchez-Portal, D. *The Journal of Chemical Physics* **2017**, *146*, 092318.

[2] Papior, N.; Lorente, N.; Frederiksen, T.; García, A.; Brandbyge, M. *Computer Physics Communications* **2017**, *212*, 8 – 24.

[3] Calogero, G.; Papior, N. R.; Kretz, B.; Garcia-Lekue, A.; Frederiksen, T.; Brandbyge, M. *Nano Letters* **2019**, *19*, 576–581.

[4] Kolmer, M.; Brandimarte, P.; Lis, J.; Zuzak, R.; Godlewski, S.; Kawai, H.; Garcia-Lekue, A.; Lorente, N.; Frederiksen, T.; Joachim, C.; Sanchez-Portal, D.; Szymonski, M. *Nature Communications* **2019**, *10*, 1573.

Poster Session Two

A novel hydrogen peroxide biosensor based on graphite electrode modified by multiwall carbon nanotube with hydroxyapatite nanoparticles

Antonio Díaz Barrios[1]
Andrés Moreno-Barreno[1], Gottfried Suppan Flores[1], Gema González Vásquez[2,3], Patricio Espinoza Montero [4] , Lenys Fernández [4]

[1] *School of Chemical Science and Engineering, Yachay Tech University, Urcuquí, Ecuador*

[2] *School of Physical Sciences and Nanotechnology, Yachay Tech University, Urcuquí, Ecuador*

[3] *Instituto Venezolano de Investigaciones Científicas (IVIC), Apartado 20632, Caracas 1020-A, Venezuela*

[4] *Escuela de Ciencias Químicas, Facultad de Ciencias Exactas y Naturales, Pontificia Universidad Católica del Ecuador, Avenida 12 de Octubre y Roca, 17-01-2184, Quito, Ecuador*

adiaz@yachaytech.edu.ec

The development of a new electrochemical biosensor that is simple, economic, reliable and highly sensitive for the detection of hydrogen peroxide by the action of Prussian Blue (PB) is presented. This sensor is based on graphite electrode modified by multiwalled carbon nanotubes (MWCNT) with hydroxyapatite nanoparticles. Prussian blue (PB), an artificial peroxidase enzyme, was successfully electrochemically deposited onto the surface of the modified electrode by the use of chronoamperometry technique. As final step the electrode was covered by poly (diallyldimethylammoniumchloride) (PDDA) to generated electrostatic stability of the sensor assembly. The modified electrode exhibits an excellent catalytic response to reduction of hydrogen peroxide.

Zinc Removal Using Magnetic Composite Materials Obtained from Lignocellulosic Waste

Salomé Galeas-Hurtado
Christopher Asimbaya, Nelly Rosas, and Víctor H.Guerrero
[1] *Escuela Politécnica Nacional, Ladrón de Guevara E11-253, Quito, Ecuador*
salome.galeas@epn.edu.ec

Magnetic composites, obtained by impregnation of magnetite nanoparticles in lignocellulosic waste were used for zinc removal from synthetic solutions. Laurel, canelo and eucalyptus sawdust, with a particle size between 74 and 150 μm were used as support. Magnetite nanoparticles were synthesized by coprecipitation at 35°C, 1.250 min^{-1} stirring and inert atmosphere. Lignocellulosic residues were added at the same conditions to obtain the composites at a rate of 1:1. X-ray Diffraction (XRD), Fourier Transform Infrared Spectroscopy (FTIR) and Scanning Electron Microscopy (SEM) confirmed the presence of magnetite nanoparticles in the lignocellulosic support. Transmission Electron Microscopy (TEM) showed nanoparticles with diameters of about 20 nm. The maximum removal amounts for 7 g/L of laurel, canelo and eucalyptus magnetic composites were 98,95; 98,80 and 97,61 %, respectively. For lignocellulosic waste alone, the maximum removal were 60,98; 46,01 and 33,31 %, respectively. Analysis adsorption isotherms determined that laurel and canelo composites fit the Freundlich model, while eucalyptus fits the Langmuir model.

References

[1] Abdolali, A.; Guo, W.; Ngo, H.; Chen, S.; Nguyen, N.; Tung, K. *Bioresource Technology* **2014**, *160*, 57–66.

[2] others„ et al. *World Applied Sciences Journal* **2013**, *28*, 1518–1530.

[3] Kapur, M.; Mondal, M. K. *Desalination and Water Treatment* **2015**, *57*, 12620–12631.

[4] Nethaji, S.; Sivasamy, A.; Mandal, A. *Bioresource Technology* **2013**, *134*, 94–100.

[5] Setyono, D.; Valiyaveettil, S. *ACS Sustainable Chemistry & Engineering* **2014**, *2*, 2722–2729.

[6] Shah, J.; Jan, M. R.; Khan, M.; Amir, S. *Desalination and Water Treatment* **2015**, *57*, 9736–9744.

[7] Zhang, Y.; Zheng, R.; Zhao, J.; Zhang, Y.; keung Wong, P.; Ma, F. *BioMed Research International* **2013**, *2013*, 1–7.

Ab initio studies of rutile TiO_2(110) pristine and defective surfaces, and the role of strong electronic correlations

Jennifer A. Sánchez
Henry P. Pinto
CompNano Group, School of Physical Sciences and Nanotechnology, Yachay Tech University, Urcuquí-Ecuador
jennifer.sanchez@yachaytech.edu.ec

TiO2 surfaces have show outstanding properties in the study of transition metal oxides, giving important results in processes such as: CO oxidation, selective propane oxidation, hydrogenation, water adsorption and other catalytic and photocatalytic oxidation reaction.[1] TiO_2 study has provided promising capabilities, able to extend to industrial purposes like high-efficiency solar cells, photocatalysts, and storage capacitors.[2] As it is known, the weakness of the standard density-functional theory (DFT) calculations on the rutile TiO_2 electronic structure is the underestimation of the band gap.[2] Hybrid functionals provide correct results, with respect to the standard methods, but this do not compensate the computational cost that it implies[3] and it makes impractical when big supercells are studied. The DFT with on-site Hubbard U corrections (DFT+U) have been tested, providing reliable structural, electronic, vibrational and thermodynamic properties of rutile TiO_2 . DFT+U consists in an explicit treatment of electronic correlations, adding an Hubbard-like term, focusing on the strong on-site Coulomb interaction of localized electrons. DFT+U implementation improve the resulting energies, electronic and magnetic properties of semiconducting materials, that contain transition metals.[2] In this work we investigate different functionals combined with Hubbard U corrections to get a good description of the electronic structure of bulk and the TiO_2 (110) surface; based on these results, the best approximation will be used to study the effect of surface oxygen vacancies and hydroxylated surface

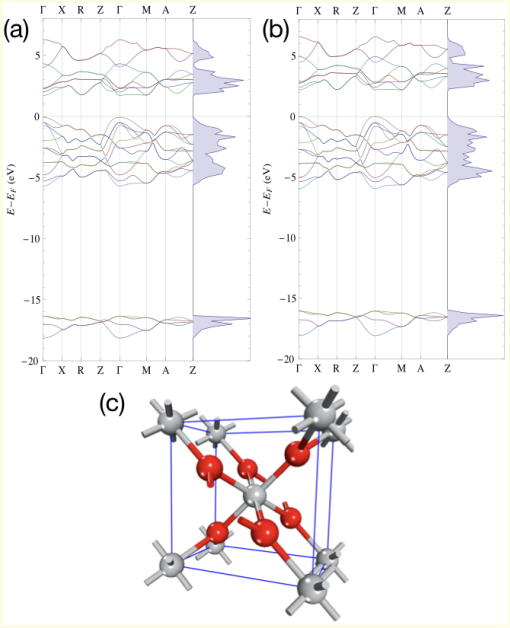

Figure 40. DFT computed band structure of bulk rutile TiO_2 using (a) PBE and (b) PBE+U(3) corrections. The predicted band gap for PBE (PBE+U(3)) is 1.7 (2.3) eV vs the experimentally observed 3 eV. (c) Crystal structure of rutile TiO_2, the red (grey) spheres represent the O (Ti) atoms; the blue lines delimits the unit cell

References

[1] Mikolajczyk, A.; Pinto, H.; Gajewicz, A.; Puzyn, T.; Leszczynski, J. *Current topics in medicinal chemistry* **2015**, *15*, 1859–1867.

[2] German, E.; Faccio, R.; Mombrú, A. W. *Journal of Physics Communications* **2017**, *1*, 055006.

[3] Hu, Z.; Metiu, H. *The Journal of Physical Chemistry C* **2011**, *115*, 5841–5845.

Experimental and Theoretical study of hybrid chitosan/ZnO with novel luminescence properties

Jose Luis Cuevas
M. Pulgar, and Gema Gonzalez
School of Physics and Nanotechnology, Yachay Tech University, Urcuquí, Ecuador
jlcuevas@yachcaytech.edu.ec
ggonzalez@yacahytech.edu.ec

Looking for new materials with different applications we have developed thin films composites based on chitosan doped with ZnO trying to obtain a synergistic effect between the components. The materials were prepared by solution casting and structural characterization was performed by SEM,FTIR and XRD. Photoluminescence properties were measured with an UV diode ((λ =385nm) as excitation source. An important increase in emission intensity was found in the materials with ZnO combinations, with an increase in the emission peak up to 530% with respect to pure chitosan. The structural and electronic properties of the chitosan/ZnO were calculated by DFT implemented in the SIESTA package.

Figure 41. Schematic representation of ZnO surface doped with chitosan

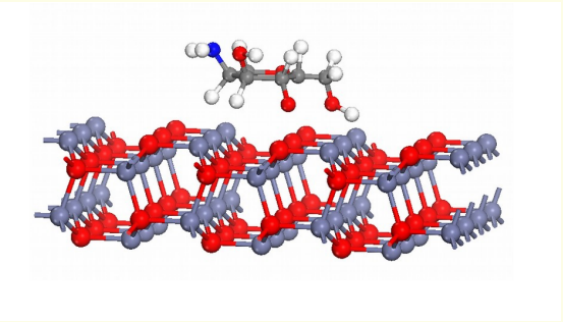

References

[1] AbdElhady, M. *International journal of carbohydrate chemistry* **2012**, *2012*.

[2] Sunil, D. Recennt advances on Chitosan-Metal Oxide Nanoparticles and their biological Application. Materials Science Forum. 2013; pp 99–108.

LCAO-TDDFT in the optical limit – Implementation and Applications

Keenan Lyon[1]
Duncan J. Mowbray[2]
[1] *Department of Applied Mathematics, University of Waterloo Waterloo, ON, Canada*
[2] *School of Physical Sciences and Nanotechnology, Yachay Tech University, Urcuquí 100119, Ecuador*
keenan.lyon@uwaterloo.ca duncan.mowbray@gmail.com

We present here an implementation within the GPAW code for Linear Combination of Atomic Orbitals (LCAO) mode Time Dependent Density Functional Theory (TDDFT) in the frequency domain in the optical limit,[2] along with benchmarking done on a selection of materials in 1D, 2D, and 3D to showcase the advantages and limitations of the code. TDDFT allows for the calculation of the dynamic/opto-electronic properties of various crystalline systems, while implementation of the LCAO mode allows for faster computation for larger systems. These calculations are also done in the exact optical limit, yielding response functions that are only dependent on frequency, a useful tool towards applications in photonics. As transition intensities are directly calculated in the LCAO-TDDFT code, the electron and hole densities can be determined for a given position and energy. With various experimental methods like electron energy loss spectroscopy (EELS) now able to probe electron excitations with atomic-scale resolution,[3] our code will allow for direct comparison with experimental results for opto-electric properties. Ultimately, we present a fast alternative to other TDDFT codes along with added functionalities useful towards applications in photonics and materials science.

Figure 42. LCAO-TDDFT code in the optical limit can be used to better understand the dynamic properties of carbon nanotubes, with their low-dimensionality and crowded unit cells proving to be a challenge for other TDDFT codes. Figure from [1]

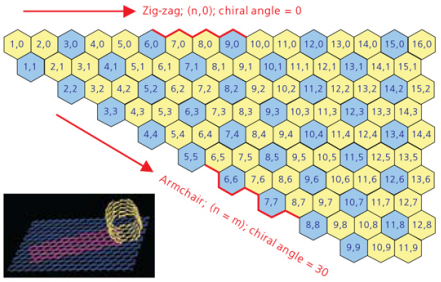

Figure 43. By not including local field effects, the LCAO mode allows for calculations of the electron and hole densities at a given position and energy. For example, in a cross-section of a graphene crystal (shown here), the relevant transitions can be determined spatially.

References

[1] Jansen, R.; Wallis, P. https://www.sigmaaldrich.com/technical-documents/articles/materials-science/single-walled-carbon-nanotubes.html, Accessed: Feb. 2019.

[2] Glanzmann, L. N.; Mowbray, D. J.; Figueroa del Valle, D. G.; Scotognella, F.; Lanzani, G.; Rubio, A. *The Journal of Physical Chemistry C* **2016**, *120*, 1926–1935.

[3] Kapetanakis, M. D.; Zhou, W.; Oxley, M. P.; Lee, J.; Prange, M. P.; Pennycook, S. J.; Idrobo, J. C.; Pantelides, S. T. *Phys. Rev. B* **2015**, *92*, 125147.

Quantum Dot Spectroscopy of Topological Rashba Nanowires

Juan Daniel Torres-Luna[1]
Denis Chevallier [2]
[1] *Department of Physics, Yachay Tech University, Hacienda San Miguel, Urcuquí, Ecuador.*
[2] *University of Basel, Klingelbergstrasse 82, CH-4056 Basel, Switzerland.*
juan.torres@yachaytech.edu.ec
denis.chevalier@unibas.ch

In condensed matter physics, Majorana fermions (MFs) are quasiparticles with non-Abelian statistics making them good candidates for topological quantum computing. We study first a one-dimensional Rashba nanowire in proximity with an s-wave superconductor and in presence of an external magnetic field.[1] By tuning the parameters of the system such as the chemical potential, we can bring it in the topological phase where MFs emerge as zero-energy modes at the edges.[2] We then propose a spectroscopy experiment to study the intrinsic properties of such particles using a quantum dot (QD). To do so, a QD is built within the same nanowire by applying an external gate. Tuning this gate allows us to probe the topological section in energy and in spin. This way to create a quantum dot is not 100% efficient because the control on the position and the width of the quantum dot is far from being perfect meaning that a normal section of the nanowire can be present between the quantum dot and the topological section. Our main goal is to study the interaction between the quantum dot states and the Andreev bound states living in this normal section and understand how they spoils the spectroscopy.

Figure 44. Local Density of States at zero energy. Localized states appear at the edge of the wire in the topological phase.

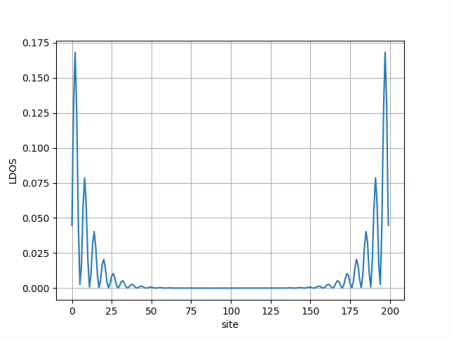

Figure 45. Structure of the gap as function of chemical potential. Andreev bound states and QD states appear inside the gap.

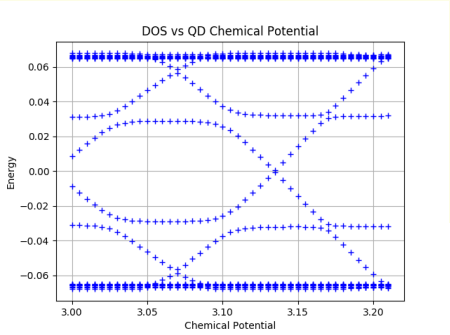

References

[1] Szumniak, P.; Chevallier, D.; Loss, D.; Klinovaja, J. *Phys. Rev. B* **2017**, *96*, 041401.

[2] Chevallier, D.; Klinovaja, J. *Phys. Rev. B* **2016**, *94*, 035417.

Figure 46. A semiconducting Rashba nanowire. It is partially covered by a s-wave superconductor. A quantum dot is built within the normal part of the wire. An external magnetic field is applied in the x-axis.

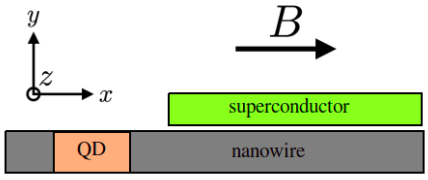

Theoretical Spectroscopy Using LCAO-TDDFT-k-ω for Chlorophyll and Carbon Nanotubes

María Rosa Preciado-Rivas
Duncan J. Mowbray, and Víctor A. Torres-Sánchez
School of Physical Sciences and Nanotechnology, Yachay Tech University, Urcuquí 100115, Ecuador

maria.preciado@yachaytech.edu.ec

The development of more efficient, environmentally friendly, and inexpensive next generation organic photovoltaic cells (OPVs) is a fundamental challenge in nanotechnology. One promising way to address this problem is the computational design of systems with molecules suitable to OPVs. To understand the excitation processes undergone by these large molecules, it is necessary to have both accurate and highly efficient computational methods to describe their optical absorption spectra. However, such methods have not previously been available to do so. In this work, we have used linear combinations of atomic orbitals (LCAO) to represent the Kohn-Sham (KS) wavefunctions, and perform time dependent density functional theory (TDDFT) calculations in the frequency domain using the LCAO-TDDFT-k-ω code, to obtain the optical absorption spectra of macromolecules such as the chlorophyll monomers and dimers in the light harvesting complexes (LHCs) in green plants, carbon nanotubes and mixtures of the two. We also apply the derivative discontinuity of the exchange-correlation functional (GLLBSC) to improve their accuracy. In this way we can rely on these methods to obtain an accurate description of the optical absorption spectra with a significant reduction in computational effort. This approach opens the pathway towards the design *in silico* of the optical spectra of macromolecules for photovoltaic and photocatalytic applications.

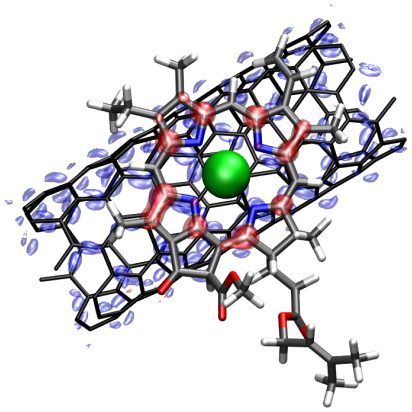

Figure 47. Schematics of a system with chlorophyll a and the (6, 4) single walled carbon nanotube. The carbon chain in chlorophyll a has been cut to C5H9. Mg, C, O, N, and H atoms are depicted in green, black, red, blue, and white. Isosurfaces of the electron (blue) and hole (red) densities $\rho(r) = \pm$ 1.0 x 10^{-6} e/Å of the first excitation of the system are shown.

References

[1] Larsen, A. H.; Vanin, M.; Mortensen, J. J.; Thygesen, K. S.; Jacobsen, K. W. *Physical Review B* **2009**, *80*.

[2] Glanzmann, L. N.; Mowbray, D. J.; del Valle, D. G. F.; Scotognella, F.; Lanzani, G.; Rubio, A. *The Journal of Physical Chemistry C* **2016**, *120*, 1926–1935.

[3] Kuisma, M.; Ojanen, J.; Enkovaara, J.; Rantala, T. T. *Physical Review B* **2010**, *82*.

First-principles studies of the electronic and mechanical properties of α-Al/γ-Al_2O_3(111) interface

Edwin M. Vásconez[1]
Jerzy Leszczynsk[2], Henry P. Pinto[1]
[1] *CompNano Group, School of Physical Sciences and Nanotechnology, Yachay Tech University, Urcuqui-Ecuador*
[2] *Department of EECS, the University of Tennessee, Knoxville, USA.*
edwin.vasconez@yachaytech.edu.ec

The gamma alumina phase γ-Al_2O_3 is mainly used in the catalysis, electronics and automotive industries due to its interesting electronic and mechanical properties.[1,2] Recent experiments on multilayered α-Al/γ-Al_2O_3 are found to exhibit improvement of the mechanical properties in comparison with individual layers.[2] However, the actual atomic structure of γ-Al_2O_3 is little known and has motivated a large number of experimental and theoretical studies.[3] The proposed study will start considering the γ-Al_2O_3 bulk structure that was already predicted using density-functional theory (DFT)[4] (see Fig. 1). Interestingly, this model predicted the formation of nanofacets on a particular surface that has been already confirmed experimentally.[1,4]
The knowledge on these surfaces is applied in the construction of a model for α-Al/γ-Al_2O_3(111) interface (cf. Fig. 2). The study will consider the interface atomic reconstruction of the metal/oxide interface which structure will be resolved using simulated annealing. The electronic and mechanical properties of the multilayered structure obtained will be computed and analyzed in the light of available experimental data.

Figure 48. DFT computed structure of γ-Al_2O_3 with $C2/m$ symmetry; the blue, red and grey spheres represent the Al, O, and Al-vacancy sites (V_{B1} and V_{B2}).

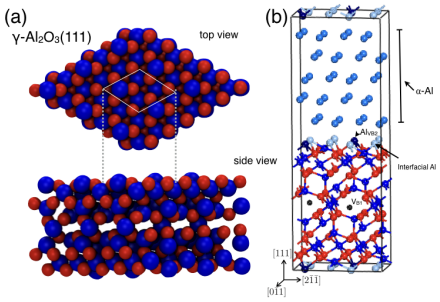

Figure 49. (a) DFT computed atomic structure of γ-Al_2O_3(111) surface. (b) Proposed model for layered α-Al/γ-Al_2O_3(111) system, the image shows the position of the interfacial Al (light blue spheres) as well as the Al vacancy sites V_B.

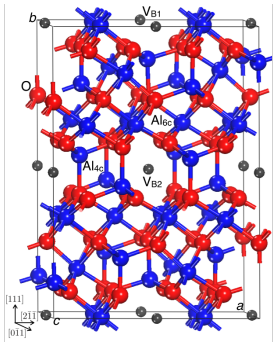

References

[1] Kovarik, L.; Bowden, M.; Genc, A.; Szanyi, J.; Peden, C. H.; Kwak, J. H. *The Journal of Physical Chemistry C* **2014**, *118*, 18051–18058.

[2] Goswami, R.; Pande, C.; Bernstein, N.; Johannes, M.; Baker, C.; Villalobos, G. *Acta Materialia* **2015**, *95*, 378–385.

[3] Digne, M.; Sautet, P.; Raybaud, P.; Euzen, P.; Toulhoat, H. *Journal of Catalysis* **2004**, *226*, 54–68.

[4] Pinto, H. P.; Nieminen, R. M.; Elliott, S. D. *Physical review b* **2004**, *70*, 125402.

Poultry Feathers Keratin: its use in the synthesis and functionalization of silver nanoparticles

Emerson Mena-Villalta
Floralba López González
Yachay Tech University, Urcuquí, Ecuador
emerson.mena@yachaytech.edu.ec
flopez@yachaytech.edu.ec

Poultry feather keratin is an unexploited natural resource of renewable protein that has many applications, including its use for synthesis and functionalization of silver nanoparticles (Ag-NPs). Keratin has a high content in the amino acid cysteine, which is connected into proteins by disulphide bonds. When keratin is dissolved the disulphide bonds are broken and the thiols are made available for the purpose of the nanoparticles synthesis. It is assumed that the free electrons of the sulphur atoms could participate in the reducing mechanism of silver in the Ag-NPs synthesis, and also due to the tail that is attached to the sulphur atom, it can also act as a capping agent, making for a uniform growth of the particles by controlling the size and shape of NPs. The most challenging part, in order to use the poultry feather waste, is the dissolution of the keratin protein because this protein has a tertiary structure; therefore, it has a great stability under normal conditions. In order to break the tertiary structure, urea is needed to denatures the protein by weakening the intermolecular bonds and interactions making the unfolding occur. Once unfolded, sodium dodecyl sulphate (SDS) is used to stabilize the unfolded structure of the protein, allowing that intermolecular bonds remain broken. And by using sodium sulphide (Na2S) to break the disulphide bonds, the complete unfolding of the structure is achieved and the keratin is maintained in solution. SEM and UVVis techniques were used to characterized the resolution solutions containing keratin capped Ag-NPs. The synergy between the great biological compatibility of keratin and the well-known bactericide effect of Ag-NPs allows the use of the obtained systems in the preparation of functional materials with promising applications.

Figure 50. : UV/Vis spectrum of silver nanoparticles synthesized with extracted keratin

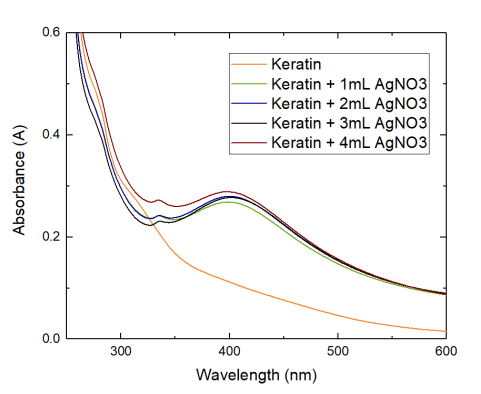

Figure 51. SEM taken of a sample containing silver nanoparticles in a keratin embedded matrix

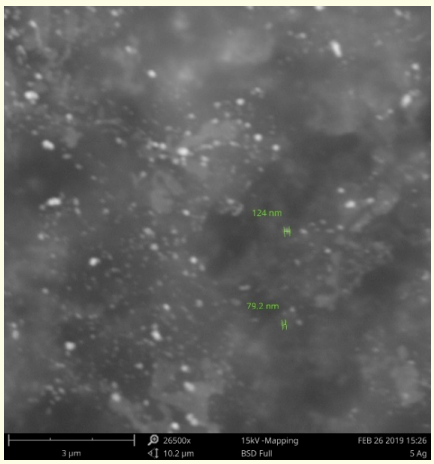

References

[1] Gupta, A.; Kamarudin, N.; Kee, C.; Yunus, R. *Journal of Chemistry & Chemical Engineering* **2012**, *6*, 732–737.

[2] Shavandi, A.; Silva, T. H.; Bekhit, A. A.; Bekhit, A. E. D. A. *Biomaterials Science* **2017**, *5*, 1699–1735.

[3] Bendit, E.; Ross, D. *Applied Spectroscopy* **1961**, *15*, 15–17.

Ab initio studies of ultra-thin CaF_2 layer on the Si(100) surface

Joshua M. Salazar[1]
Damien Riedel [2], Henry P. Pinto [1]
[1] *CompNano Group, School of Physical Sciences and Nanotechnology, Yachay Tech University, Urcuqui-Ecuador*
[2] *Institut des Sciences Moléculaires d'Orsay, ISMO, UMR 8214, CNRS, Université Paris Sud, 91405 Orsay Cedex, France*
joshua.salazar@yachaytech.edu.ec

Molecular electronics development requires the effective electronic isolation of a given molecule with the substrate as well as a precise atomic manipulation.[1] In this work, we study the CaF_2 /Si(100) interface that it is currently used for electronic manipulation of molecules at the nanoscale. This interface has been already grown experimentally for certain coverage regime.[2,3] Unfortunately, to the best of our knowledge, an accurate description of the stripe formation of CaF_2 /Si(100) interface remains unsolved.[3] In order to solve this problem, we propose a theoretical study of this interface using density-functional theory (DFT) to obtain the electronic structure and the most likely atomic configurations of the interface. The generalized gradient approximation functionals tend to fail when describing the correct cohesive energies between the layers in this kind of systems. To accurately simulate such systems it is needed to take into account the weak van der Waals interactions arising between the CaF_2 and the Si(100) surface. In this work, we will use van der Waals density functional (vdW-DF) approach.[4] Employing this functional, we investigate the configuration and energetics of several interfaces, the simulated scanning tunneling microscopy (STM) images of the most stable interfaces will be generated and compared directly with the experiment.

Figure 52. vdW-DF computed partial density of states of likely CaF_2 /Si(100) stripe structure. On the left is displayed the corresponding atomic surface structure where the yellow, cyan and green spheres represent the Si, F and Ca atoms, respectively.

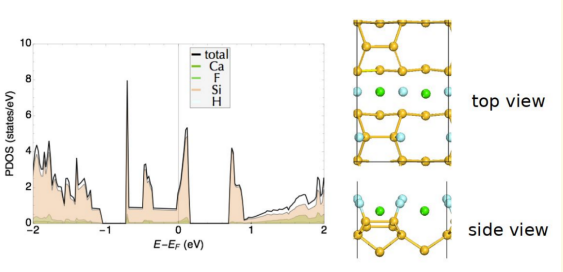

Figure 53. Theory vs experiment of CaF_2 /Si(100) stripe structure: (a) Simulated STM image of structure displayed in Fig 52. with a bias voltage of -2.0 V. (b) Experimental STM image with bias voltage of -2.0 V. The surface unit cell is displayed in both cases for comparison.

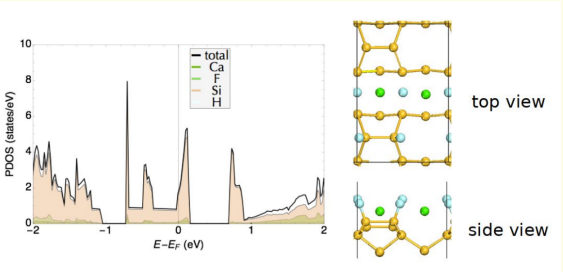

Acknowledgments
Special thanks to the Park Systems company for funding this research poster presentation at the International Edition of the Nanoscience Summer School @ Yachay 2019 in Galapagos.

References

[1] Colton, R. J. *Journal of Vacuum Science & Technology B: Microelectronics and Nanometer Structures Processing, Measurement, and Phenomena* **2004**, *22*, 1609–1635.

[2] Chiaravalloti, F.; Dujardin, G.; Riedel, D.; Pinto, H. P.; Foster, A. S. *Physical Review B* **2011**, *84*, 155433.

[3] Chiaravalloti, F.; Dujardin, G.; Riedel, D. *Journal of Physics: Condensed Matter* **2014**, *27*, 054006.

[4] Rydberg, H.; Dion, M.; Jacobson, N.; Schröder, E.; Hyldgaard, P.; Simak, S.; Langreth, D. C.; Lundqvist, B. I. *Physical review letters* **2003**, *91*, 126402.

Electronic and atomic structure of NbS_2 intercalated with Li

Jorge D. Vega[1]
Damien Voiry[2], Henry P. Pinto[1]
[1] *CompNano Group, School of Physical Sciences and Nanotechnology, Yachay Tech University, Urcuquí-Ecuador*
[2] *Institut Européen des Membranes (IEMM, ENSCM UM CNRS UMR5635), Montepellier-France*
jorge.vega@yachaytech.edu.ec

NbS_2 is a transition metal dichalcogenide. Some experiments on bulk and thin films of NbS_2 have shown remarkable features such as superconductivity and metallic transport properties.[1,2] In addition, this material has promising applications in quantum engineering, i.e. miniaturized neuromorphic computing. NbS_2 intercalated with Li ($LiNbS_2$) is a novel material that present interesting electronic properties but there are scarce theoretical studies to understand the material's properties and behaviour.[1] We have performed ab initio calculations using density-functional theory (DFT) to study the electronic structure of bulk NbS_2 and $LiNbS_2$ as well as the of $LiNbS_2$ (001) surface. The calculations were performed with the strongly constrained and appropriately normed semilocal (SCAN) density functional including van der Waals interactions[3] that is suitable for these layered compounds (cf. Fig 54). The density of states, simulated photoelectron spectroscopy, scanning tunneling microscopy (STM) images and phonon band structure are studied in detail and compared with experiments.

Figure 54. Partial density of states of bulk LiNbS2 calculated with SCAN+vdW functional. The cyan (yellow) part corresponds to Niobium (sulfur)'s density. The partial density of Li in violet is almost imperceptible. The DFT calculations predict the bulk $LiNbS_2$ as semiconductor. The bulk structure is displayed in the inset.

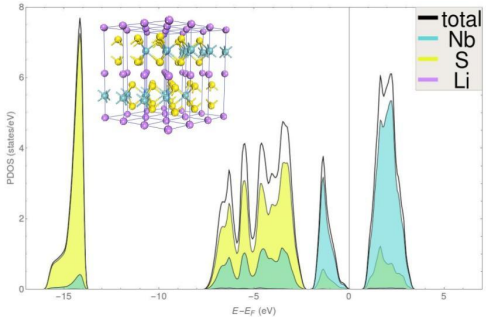

Figure 55. SCAN+vdW computed STM image for $LiNbS_2$(001) surface for bias voltage of -0.7 V. The bright (dark) protrusions are located on the surface S (subsurface Nb). The predicted lattice is superimposed on the image where the yellow and cyan spheres represent the S and Nb atoms, respectively. The blue lines delimits the surface unit cell.

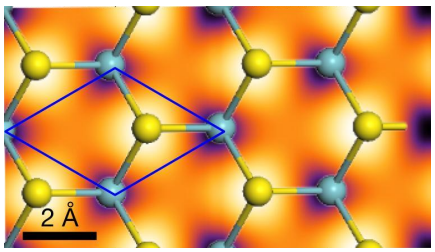

References

[1] van Loon, E. G.; Rösner, M.; Schönhoff, G.; Katsnelson, M. I.; Wehling, T. O. *npj Quantum Materials* **2018**, *3*, 32.

[2] Kuc, A.; Zibouche, N.; Heine, T. *Physical Review B* **2011**, *83*, 245213.

[3] Sun, J.; Ruzsinszky, A.; Perdew, J. P. *Physical review letters* **2015**, *115*, 036402.

Ab initio calculations of bulk NiO and the NiO(100) surface, and the effect of O vacancies on the magnetic properties

Jorge D. Vega[1]
Alicja Mikolajczyk[2], Henry P. Pinto[1]
[1] *CompNano Group, School of Physical Sciences and Nanotechnology, Yachay Tech University, Urcuquí-Ecuador*
[2] *Laboratory of Environmental Chemometrics, University of Gdansk, Gdansk-Poland*
jorge.vega@yachaytech.edu.ec

NiO oxide is a technological important material because of its applications in fuel cells, gas sensors, batteries, optoelectronic devices, as a catalyst, and the others.[1] From a theoretical perspective, this transition metal oxide presents challenges for the conventional density-functional theory (DFT) methods. DFT simulations have been developed in order to understand the electronic structure and other properties such as the bulk modulus, the equation of state, the band gap, and magnetism of the bulk rock salt of Nickel Oxide (NiO), as well as NiO surfaces. The calculations were performed with the strongly constrained and appropriately normed semilocal (SCAN) density-functional[2] including on-site Hubbard U corrections for the Ni-3d within the Dudarev approach.[3] In addition, some calculations of the bulk ferromagnetic and nonmagnetic phases of NiO are analyzed, showing up why the antiferromagnetic phase is the most stable. SCAN+U calculation on the pristine (cf. Fig 56) and defective NiO(100) surface are presented. The effect of surface and subsurface oxygen vacancies on the surface magnetization is computed. Simulated photoelectron spectroscopy, formation energies and scanning tunneling microscopy are analyzed on the light of experimental data.

Figure 56. Atomic structure of rock salt NiO with antiferromagnetic order. The atoms in red, blue and orange are oxygen, Ni with magnetic moment +m, and Ni with magnetic moment −m, respectively.

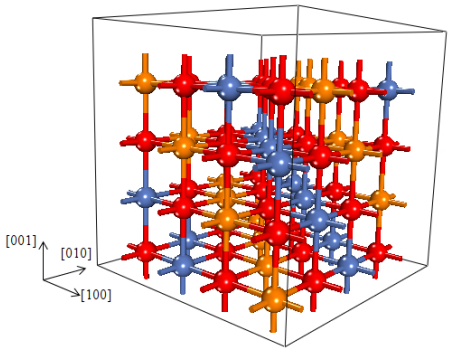

Figure 57. (a) Topographic-mode empty states STM image of NiO(100) obtained experimentally. The bright regions locate the Ni positions and the dark regions the O positions. Corrugation heights (CH) are shown as horizontal linescans taken through the center of the images. b) DFT-SCAN+U(4) computed empty states STM images of NiO(100). The bright (dark) regions locates the Ni (O) position.

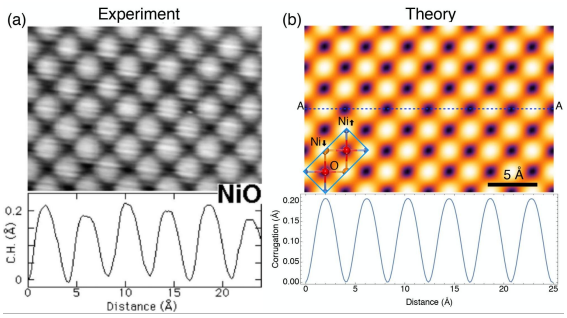

References

[1] Srinivasaraghavan, R.; Chandiramouli, R.; Jeyaprakash, B.; Seshadri, S. *Spectrochimica Acta Part A: Molecular and Biomolecular Spectroscopy* **2013**, *102*, 242–249.

[2] Sun, J.; Ruzsinszky, A.; Perdew, J. P. *Physical review letters* **2015**, *115*, 036402.

[3] Dudarev, S.; Botton, G.; Savrasov, S.; Humphreys, C.; Sutton, A. *Physical Review B* **1998**, *57*, 1505.

Cytotoxicity prediction of organic molecules using electronic structure simulations and quantitative structure-activity relationships modeling

Doménica R. Bermeo[1]
Alicja Mikolajczyk[2], Yadira F. Ordonez[3],Mireia Casasampere[4], Henry P. Pinto[1]
[1]*CompNano Group, School of Physical Sciences and Nanotechnology, Yachay Tech University, Urcuquí-Ecuador*
[2] *2Laboratory of Environmental Chemometrics, University of Gdansk, Gdansk-Poland*
[3]*BIONAP, Escuela de Ciencias Agrícolas y Ambientales, Pontificia Universidad Católica del Ecuador Sede Ibarra, Ibarra-Ecuador*
[4]*CSIC, Institut de Quimica Biomedica, RUBAM, Barcelona-Spain*
domenica.bermeo@yachaytech.edu.ec

Electronic structure simulations and quantitative structure-activity relationships modeling (QSAR) has been successfully applied to predict toxicity of chemical compounds without expensive and time-consuming experiment with use of animal testing.[1] These computational methods could provide a sophisticated approach to accelerate the discovery and production of new chemical compounds targeted to specific needs that could be of interest in the developed of pharmaceuticals and industrial chemicals. Recent studies on the biological activity of these set of compounds (see Fig. 58) have shown promising cytotoxicity when applied on brain cancer cells. Those compounds induce cell death by either apoptosis or autophagy.[2] Inspired by those promising experimental results, we present here a QSAR modeling capable of predicting the LD_{50} of the already tested organic molecules. Specifically, we will employ rigorous quantum mechanics calculations using density-functional theory within the B3LYP approximation to obtain the electronic structure of the molecules; the conformers of each molecule will be explored with a semiempirical quantum mechanical method and finally a predictive QSAR model will be developed to describe relationship between structure and cytotoxicity effect of tested organic molecules. The developed QSAR model as well as obtained electronic structure properties will be then applied to predict the cytotoxicity effect of similar molecules without the need of experiments. In result we expect that the design process of new tested chemicals for brain cancer therapy will be faster, cheaper and more efficient.

Figure 58. Sketch of organic molecules to be analyzed. a) Phenoxodiol ,b)Gamma-tocotrienol ,c) Celecoxib and d) Resveratrol.

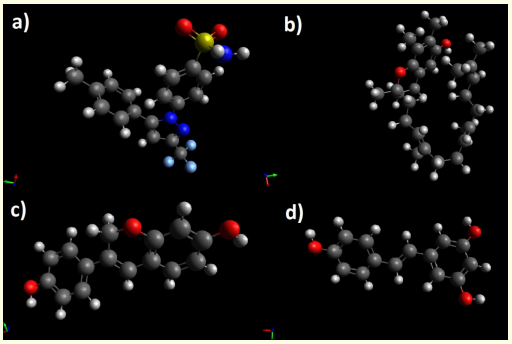

References

[1] Puzyn, T.; Rasulev, B.; Gajewicz, A.; Hu, X.; Dasari, T. P.; Michalkova, A.; Hwang, H.-M.; Toropov, A.; Leszczynska, D.; Leszczynski, J. *Nature Nanotechnology* **2011**, *6*, 175–178.

[2] Casasampere, M.; Ordóñez, Y. F.; Casas, J.; Fabrias, G. *Biochimica et Biophysica Acta (BBA) - General Subjects* **2017**, *1861*, 264–275.

Computational Studies of Graphene Flower-like Superlattices

Doménica N. Garzón
Jorge D. Vega, and Henry P. Pinto
CompNano Group, School of Physical Sciences and Nanotechnology, Yachay Tech University, Urcuquí-Ecuador
domenica.garzon@yachaytech.edu.ec

Graphene has been widely studied in recent years and it is a prospective material for nanoelectronics. In order to identify the different applications of graphene, a deep study of its characteristics and properties is necessary, including defects as it is known that they can influence on the chemical, mechanical, and electronic properties of graphene.[1] One class of those defects are topological, i.e., grain boundary loops (GBL). Recently, it has been observed through scanning tunneling microscopy (STM) flower-like patterns, which could form superlattices. In this context, a systematic study of structural, mechanical, electronic and magnetic properties of graphene with flower-like defects (FLD) is relevant for future applications. Recent measurements suggests that some of these one-dimensional extended topological defects can have unique electronic properties, such as a one-dimensional conductivity.[2] Inspired in the experimental evidence of FLD, we propose and investigate a hypothetical system formed by a hexagonal array of such flower-like defects with different separations forming a superlattice. Using density-functional theory within the meta-GGA approximation provides a high level of accuracy and flexibility in the simulation of the properties of these superlattices. Atomic and electronic structure, formation energies, scanning tunneling microscopy images, and the effect of carbon vacancies on the magnetic properties of these superlattices will be computed and analyzed.

Figure 59. Computed C6(1,1)-(10x10) superlattice (a) partial density of states (PDOS) for the FLD (pristine) region in green (blue), the superlattice structure is displayed on the top left. (b) STM images for different bias voltages. (c) close-up of STM image for v= +0.3 V and (d) shows a larger view of the hexagonal patterned superlattice. The blue line denotes the unit cell of the displayed structure

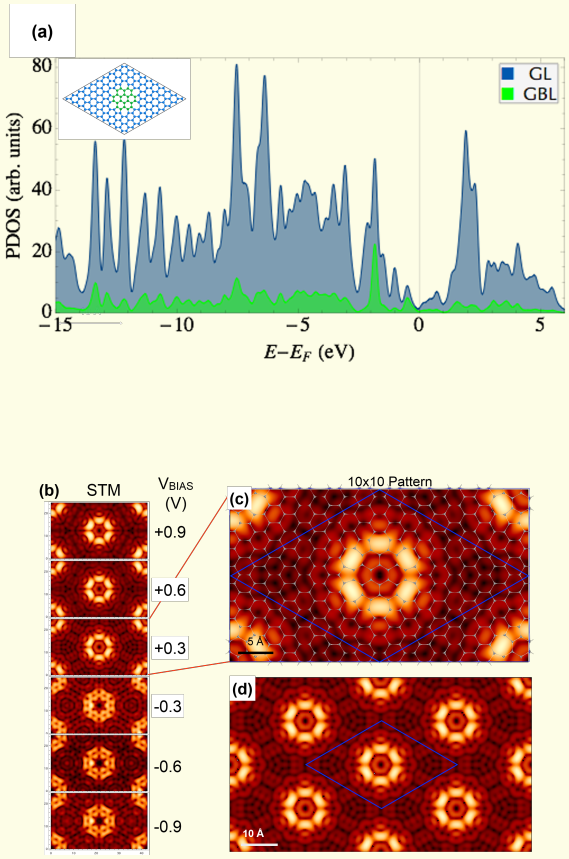

References

[1] Cockayne, E.; Rutter, G. M.; Guisinger, N. P.; Crain, J. N.; First, P. N.; Stroscio, J. A. *Phys. Rev. B* **2011**, *83*, 195425.

[2] Pinto, H.; Leszczynski, J. *Fundamental Properties of Graphene, Handbook of Carbon Nano Materials*; World Scientific, 2014.

Synthesis and characterization of cellulose-based hydrogels for antibiotic delivery against Leishmaniasis

Carolina Serrano-Larrea[1]
Frank Alexis[1], Javier Santamaría-Aguirre[2,3]
[1] *School of Biological Sciences and Engineering, Yachay Tech, San Miguel de Urcuquí, Ecuador*
[2] *Instituto de Investigación en Salud Pública y Zoonosis (CIZ), Quito, Ecuador*
[3] *Universidad Central del Ecuador*
andrea.serrano@yachaytech.edu.ec

Leishmaniasis is a neglected disease caused by protozoa of the genus Leishmania. It presents three main forms, visceral, cutaneous and mucocutaneous leishmaniasis.[1] Cutaneous leishmaniasis is a public health problem in Ecuador because of its wide distribution, mainly in rural areas in the regions of Costa, Sierra and Oriente. It is present in 23 out of the 24 provinces.[2] The first-line treatment is antimonate meglumine, has a large number of adverse effects: nephrotoxicity, hepatoxicity, anorexia, headache, problems related to the musculoskeletal system and can cause death. The cost of treatment is high and is developing resistance.[1] Due to this, new alternatives are being sought such as fluoroquinolones, has been reported active on topoisomerases II of Leishmania; they has lower cost, fewer adverse effects.[3] Hydrogels based on polysaccharide natural polymers are of great interest in biomedical applications and more specifically for tissue regeneration and drug delivery.[4] The aim of this work is to develop cellulose-based hydrogels that is loaded with fluoroquinolones to have antileishmanial activity. The Hydrogels are made of different types of cellulose fibers extracted from Ecuadorian plants, depending on the cellulose fiber, we expect to see different properties on the properties of the hydrogel and fluoroquinolones release process.

Figure 60. Hydrogel formation

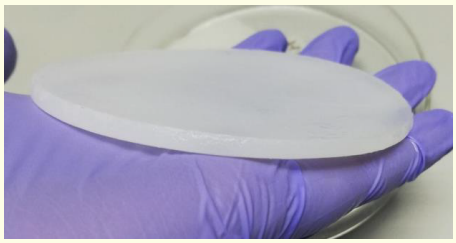

Figure 61. Leishmaniasis infection

References

[1] World of Health Organization Leishmaniasis. https://www.who.int/news-room/fact-sheets/detail/leishmaniasis, 2018.

[2] others„ et al. *BMC infectious diseases* **2006**, *6*, 139.

[3] Reguera, R. M.; Escudero-Martínez, J. M.; Domínguez-Asenjo, B.; Gutiérrez-Corbo, C.; Balaña-Fouce, R. *Drug Discovery for Leishmaniasis*; 2017; pp 348–370.

[4] del Valle, L.; Díaz, A.; Puiggalí, J. *Gels* **2017**, *3*, 27.

Chitosan Films Doped with LiClO4 and ZnO NPs as Conductive/Luminescent Polymer

Marlon Gurumendi Sánchez[1]
Gema González[1], Juan Lobos Martin[1], Floralba López [2], and Ana Rivas [3]
[1] *School of Physical Sciences and Nanotechnology, Yachay Tech University, Urcuqui, Imbabura, Ecuador*
[1] *School of Chemical Sciences and Engineering, Yachay Tech University, Urcuqui, Imbabura, Ecuador*
[2] *University of Chinese Academy of Sciences*
[3] *Faculty of Engineering in Mechanics and Production Sciences, Escuela Superior Politécnica del Litoral, Guayaquil, Guayas, Ecuador*
marlon.gurumendi@yachaytech.edu.ec

Chitosan (CS) is a biopolymer highly biocompatible, and have the capacity to accept chemical modifications with different ions that improve its ionic conductivity and its luminescence properties.[1] CS hybrid thin films containing ZnO NPs and Li ions were prepared by using solution casting method. These materials can have important applications as sensor and supercapacitors. Lithium is added to increase the ionic conductivity and ZnO for luminescence properties.[2] To follow the structural changes in the chitosan film various characterization techniques were performed. X-ray diffraction (XRD), Fourier Transform Infrared spectroscopy (FTIR), Scanning Electron Microscopy (SEM), and UV-Visible. Additionally, the ionic conductivity of the different solutions was measured by Electrochemical Impedance Spectroscopy (EIS), and photoluminescence measurements were also carried out. The addition of Li was very clearly observed in the FTIR with the presence of the vibration band at 623 cm^{-1} up to 20%. Fig. 62 showed the characteristic XRD peaks of chitosan at 11.88 and 20.41°.[1] The addition of Li in high concentration (up to 40%) induced amorphization in the chitosan membrane. The ionic conductivity of the polymer films increased with $LiClO_4$ concentrations (Fig. 63). Therefore

Figure 62. XRD of chitosan film containing 20% of $LiClO_4$ and 1% ZnO respect to the concentration of chitosan.

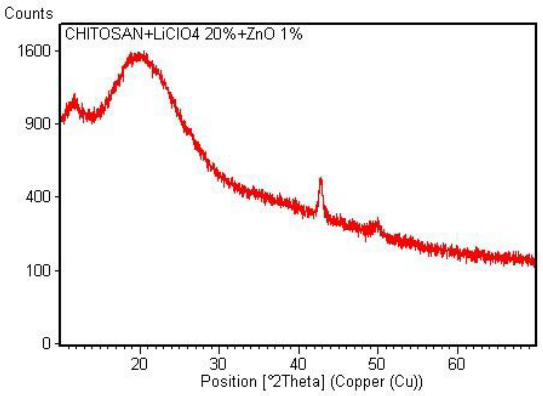

Figure 63. Nyquist diagram of (a) chitosan film and (b) chitosan containing 15% of $LiClO_4$.

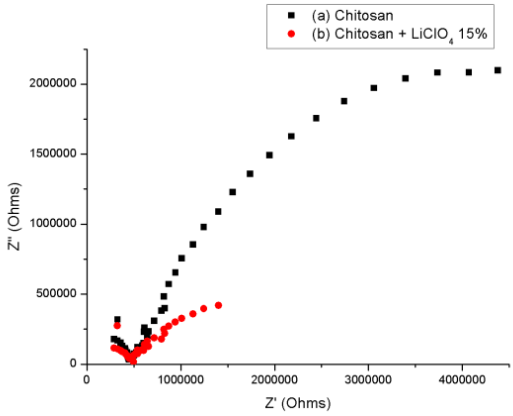

References

[1] Wang, Y.; Pitto-Barry, A.; Habtemariam, A.; Romero-Canelon, I.; Sadler, P. J.; Barry, N. P. *Inorganic Chemistry Frontiers* **2016**, *3*, 1058–1064.

[2] Fauzi, I.; Arcana, I.; Wahyuningrum, D. Synthesis and Characterization of Solid Polymer Electrolyte from N-Succinyl Chitosan and Lithium Perchlorate. Advanced Materials Research. 2014; pp 58–61.

Low-Kinetic Energy Nitrogen Ion Irradiation of vertically-aligned Carbon Nanotubes

Sebastián I. Cortez[1]
Ayrton Sierra[2], Jean-François Colomer[2], Carla Bittencourt [3], Duncan J. Mowbray [1], and Julio C. Chacón Torres[1]

[1] *Yachay Tech University, School of Physical Sciences and Nanotechnology, Urcuquí 100119, Ecuador*

[2] *Research group on carbon nanostructures (CARBONNAGe), University of Namur, Belgium*

[3] *Chemistry of Interaction Plasma Surface (ChIPS), University of Mons, Belgium*

sebastian.cortez@yachaytech.edu.ec

Currently, Nitrogen doping of carbon nanotubes is a promising route to tailor the electronic properties and the chemical reactivity of carbon nanotubes. In this work, we growth verticallyaligned carbon nanotubes via catalytic chemical vapor deposition (CCVD),[1] and doped them with nitrogen using Ion irradiation. To characterize the influence of the nitrogen doping, we combined experimental measurements and all-electron density functional theory simulations (AEDFT) of x-ray photoelectron spectroscopy (XPS).[2,3] Using these two approaches we were able to determine the different nitrogen containing species (pyridinic, pyrrolic, or graphitic) and how they vary respect to the kinetic energy of the nitrogen ions. This work shows a favorable path towards the control of the electronic properties and chemical reactivity of carbon nanotubes.

Figure 64. Scheme of the work done. The grafting of nitrogen atoms in the carbon nanotubes producing certain defects (trimerized pyridine defect), followed by XPS analysis using DFT calculations.

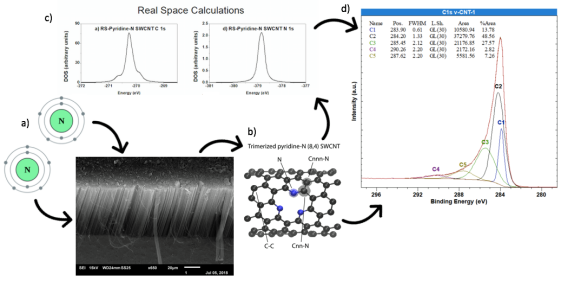

References

[1] Tran, K. Y.; Heinrichs, B.; Colomer, J.-F.; Pirard, J.-P.; Lambert, S. *Applied Catalysis A: General* **2007**, *318*, 63–69.

[2] Scardamaglia, M.; Amati, M.; Llorente, B.; Mudimela, P.; Colomer, J.-F.; Ghijsen, J.; Ewels, C.; Snyders, R.; Gregoratti, L.; Bittencourt, C. *Carbon* **2014**, *77*, 319–328.

[3] others„ et al. *The Journal of Physical Chemistry C* **2016**, *120*, 18316–18322.

Friday

Raman spectroscopy in carbon nanostructures

Ado Jorio
Departamento de Física, UFMG, Belo Horizonte,MG, Brazil – 31270-901
adojorio@fisica.ufmg.br

In this presentation, the use of Raman spectroscopy to study carbon nanostructures will be discussed (see Fig. 65), including amorphous carbon, carbon nanotubes, linear carbon chains, graphene and some other intriguing materials, such as the Terras Pretas do Índio (Indian Black Earth).[1] The technique is able not only to identify the different structures, but also to study its vibrational and electronic properties, and to characterize other physical and chemical properties, including perturbations such as doping and strain. The different aspects that enable us to measure single molecular nanospecies will be explored, including resonance effects[2] and tip enhanced Raman spectroscopy.[3]

Figure 65. Examples of Raman spectra from different carbon nanostructures, from the top to the bottom: as produced amorphous carbon, amorphous carbon heat treated at different temperatures (htT), namely 1,200 and 1,800 K; *Indian Black Earth* (TPI), graphene, highly oriented pyrolytic graphite (HOPG), single wall carbon nanotubes (SWCNT) and multiwall carbon nanotubes (MWCNT) filled with linear carbon chains.[1]

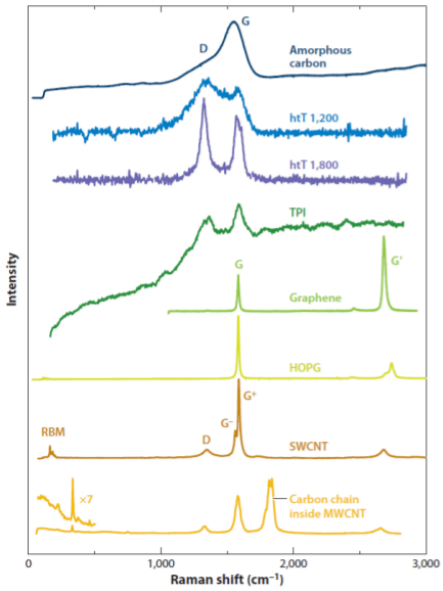

References

[1] Jorio, A.; Souza Filho, A. G. *Annual Review of Materials Research* **2016**, *46*, 357–382.

[2] Jorio, A.; Dresselhaus, M.; Saito, R.; Dresselhaus, G. Raman spectroscopy in graphene related systems, swiley. 2011.

[3] Jorio, A.; Cançado, L. G.; Heeg, S.; L.Novotny,; Hartschuh, A. *World Scientific Series on Carbon Nanoscience - Handbook of Carbon Nanomaterials*; 2019; pp 175–221.

Imaging and Spectroscopy of Two Dimensional Graphene Heterostructures

Leonardo Basile[1] L. Liu[2], G. Gu[2], W. Zhou [3], A. Lupini [4], and J. C.Idrobo[4] [1]*Escuela Politécnica Nacional, Ladrón de Guevara E11-253, Quito, Ecuador*
[2]*Department of EECS, the University of Tennessee, Knoxville, USA.*
[3] *University of Chinese Academy of Sciences*
[4] *Center for Nanophase Materials Sciences, Oak Ridge National Laboratory, Oak Ridge, USA*
leonardo.basile@epn.edu.ec

Aberration-correction in the scanning electron microscope (STEM) has allowed to correlate structural and spectroscopic data of materials at atomic resolution. In particular, we now can determine, by spectroscopic means, the chemical bonding, optical properties, individual impurities, in two dimensional materials.

In this talk, we will show our ongoing efforts to study graphene heterostructures using STEM analytical techniques. For instance, we demonstrated heteroepiaxy in two-dimensional space with a 1D sharp interface in a prototypical material system: graphene and hexagonal boron nitride (BN).[1] In Figure 66 we examined the contaminant-covered graphene-BN boundary, using electron energy-loss spectroscopy (EELS). Fast Fourier Transform of the areas shown in (A) indicates that the BN is aligned with the graphene monolayer. Evidence of a sharp interface is provided by the chemical map shown in (E), where the boron K-edge clearly defines a sharp graphene-BN interface, establishing EELS as a powerful "see-through" tool.

Figure 66. STEM-MAADF image and EELS. (A) MAADF image of a graphene-BN boundary. (B) y (C) fast Fourier transforms (FFT) of the highlighted areas shown in (A). (D) and (E) simultaneously acquired STEM image and electron energy loss spectrum map (boron K-edge) of a region containing a buried graphene-BN boundary, respectively. The blue/white dashed lines indicate the boundary between the graphene and the BN. Scale bars are 5nm.

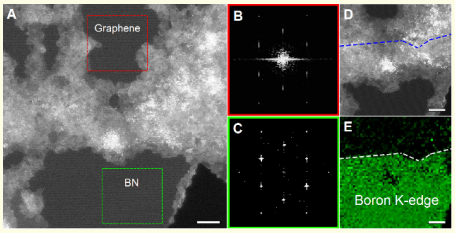

Figure 67. (Left) Experimental MAAD images of twisted bilayer graphene.(Right) EEL spectra obtained from twisted bilayer graphene samples.

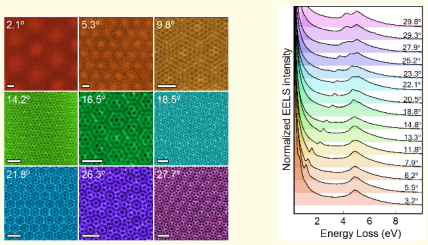

In another example, the left panel of Figure 67 shows a set of experimental medium angle annular dark field (MAADF) images of twisted bilayer graphene obtained at different misorientation angles. The Moiré patterns formed by the interference between the graphene hexagonal honeycomb lattices are clearly observed. The right panel in Figure 67 shows the respective EEL spectra acquired at different misorientation angles. A new absorption peak emerges at about 2.3 eV at misorientation angle between the graphene layers of $14°$. The new absorption peak shifts towards the infrared (ultraviolet) region of the spectra as the misorientation angle decreases (increases). The results indicate that band gap tuning could be achieved by controlling the misorientation angle in twisted bilayer graphene. Measurements were carried out in an aberration-corrected STEM, a Nion UltraSTEMTM 100, equipped with a cold field emission electron source, a corrector of third and fifth order aberrations, and a Gatan Enfina spectrometer.[2]

References

[1] Liu, L.; Park, J.; Siegel, D. A.; McCarty, K. F.; Clark, K. W.; Deng, W.; Basile, L.; Idrobo, J. C.; Li, A.-P.; Gu, G. *Science* **2014**, *343*, 163–167.

[2] Krivanek, O.; Corbin, G.; Dellby, N.; Elston, B.; Keyse, R.; Murfitt, M.; Own, C.; Szilagyi, Z.; Woodruff, J. *Ultramicroscopy* **2008**, *108*, 179–195.

Surface-enhanced spectroscopy and ultra-strong light-matter coupling

Stephanie Reich
Freie Universität Berlin
reich@physik.fu-berlin.de

Metal nanoparticles sustain pronounced resonances that arise from localized surface plasmons. Plasmons are collective oscillations of free electrons in a material that give rise to electromagnetic near fields close to the metal surface. Close to the metal, the electromagnetic field is enhanced by several orders of magnitude. Therefore, plasmonic nanoparticles are called lenses to focus light into nanoscale volumes thereby increasing its amplitude and interaction strength. Plasmons are exploited in surface-enhanced spectroscopy. Most prominent is surface-enhanced Raman scattering, where the cross section of the Raman effect increased by up to 10 orders of magnitude through plasmonic interaction. In this presentation, I will give an overview over the work on nanoplasmonics and surface-enhanced spectroscopy done in our lab. I will show how we measure enhancement factors in carefully constructed plasmonic nanostructures to learn about the nature of the enhancement. I will discuss the strong interaction between light and other degrees of freedom that is induced by the plasmon and how we can use this to realize optomechanical systems and plasmon-polaritons with giant light-matter coupling.

Molecular electronic devices based on monomolecular films

Henrry M. Osorio[1]
Santiago Martín[2],Pilar Cea[2], Paul J. Low [3], Simon J. Higgins[4], and Richard J. Nichols [4]
[1]*Departamento de Física, Escuela Politécnica Nacional, Av. Ladrón de Guevara, E11-253, 170525, Quito, Ecuador.*
[2]*Departamento de Química Física, Facultad de Ciencias, Universidad de Zaragoza, 50009 Zaragoza, Spain.*
[3] *School of Molecular Sciences, University of Western Australia, 6009 Crawley, WA, Australia.*
[4] *Department of Chemistry, University of Liverpool, L69 7ZD Liverpool, United Kingdom.*
henrry.osorio@epn.edu.ec

Molecular Electronics is an emergent technology in which organic, inorganic or organometallic molecules are connected between two (or three) electrodes (Figure 1), and their electrical properties are harnessed to perform some useful function that can translate to enhanced or novel performance in an electronic device.[1] Thus, this nascent technology emerges as candidate to replace the current complementary metal-oxidesemiconductor (CMOS) technology. However, there are a number of scientific and technological challenges that need to be addressed before molecular electronics can be implemented in the market.[2] One of these challenges is related to the incompatibility that exists between the studied single-molecule devices (metal-molecule-metal junctions, Figure 1, right) and the production of devices using large-scale fabrication techniques.[3,4] In this talk, I will describe our efforts to address this challenge using monomolecular films forming metal-organic monolayer-metal junctions (Figure 1, left). Specially, the talk will describe the experimental results that show the influence in the electrical response of a junction upon increasing the surface coverage of molecular components from truly isolated single molecules to more densely packed and ordered films.[5,6]

Figure 68. Illustration of molecular junctions formed from a single-molecule configuration, SMC, (right) and using a monomolecular film (left).

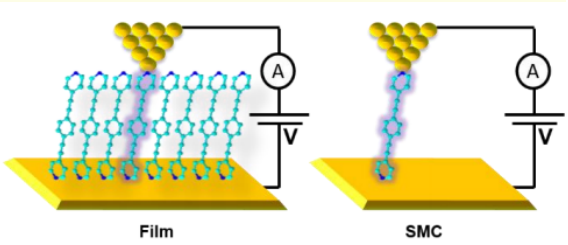

References

[1] *Nature Nanotechnology* **2013**, *8*, 377–377.

[2] *Nature Nanotechnology* **2013**, *8*, 385–389.

[3] Xiang, D.; Wang, X.; Jia, C.; Lee, T.; Guo, X. *Chemical Reviews* **2016**, *116*, 4318–4440.

[4] Osorio, H. M.; Cea, P.; Ballesteros, L. M.; Gascón, I.; Marqués-González, S.; Nichols, R. J.; Pérez-Murano, F.; Low, P. J.; Martín, S. *Journal of Materials Chemistry C* **2014**, *2*, 7348–7355.

[5] Osorio, H. M.; Martín, S.; López, M. C.; Marqués-González, S.; Higgins, S. J.; Nichols, R. J.; Low, P. J.; Cea, P. *Beilstein journal of nanotechnology* **2015**, *6*, 1145–1157.

[6] Osorio, H. M.; Martín, S.; Milan, D. C.; González-Orive, A.; Gluyas, J. B.; Higgins, S. J.; Low, P. J.; Nichols, R. J.; Cea, P. *Journal of Materials Chemistry C* **2017**, *5*, 11717–11723.

Site-controlled Nano-heteroepitaxy of GaAs on Si

Ivan Prieto[1]
O. Skibitzki, R. Kozak, G. Capellini, P. Zaumseil, E. Gini, R. Erni, M. D. Rossell, T. Schroeder, and H. von Känel
Laboratory for Solid State Physics, ETH Zürich, CH-8093 Zürich, Switzerland,
**IST Austria, Am Campus 1, Klosterneuburg, Austria*
ivan.prieto@ist.ac.at

The unique electronic and optical properties of III-V materials have attracted much attention. The integration of those materials on Si is, however, complicated by the presence of misfit dislocations, anti-phase domains and other crystal defects occurring as they exhibit different structural and thermal characteristics. The nucleation of GaAs on planar Si(001) is of three- dimensional character (Volmer-Weber mechanism).[1] Dislocation-free GaAs nuclei are predicted at an early stage of the growth as long as their size is within a few tens of nm.[2] A novel type of Si substrate consists of so called nano-tips (NTs) is presented. The NTs, formed by lithography and etching, are embedded in SiO 2 and have diameters ranging between 5-80 nm and 250-300 nm at the top and the base, respectively. Figure 69(a–b) shows a SEM view of a single NT exhibiting a 30 nm top diameter, with no surrounding oxide. An AIXTRON 200/4 metal-organic vapor phase epitaxy (MOVPE) tool was used to selectively deposit GaAs on such NTs. The sample preparation comprises a Piranha clean, HF dip and subsequent As passivation in the MOVPE tool at 720 oC. TMGa and AsH 3 sources were used as reactive gases, at a reactor pressure of 100 mbar, temperature of 570 oC and a V/III ratio of 130, leading to an effective growth rate of 0.1 nm/s. This resulting nanostructures exhibit different morphologies according to a bi-modal size distribution as revealed by a statistical analysis.[3] Some small nuclei turned out to be (001)-oriented GaAs single crystals, as verified by high resolution transmission electron microscopy (HR-TEM) and electron backscatter diffraction (EBSD). Larger nuclei exhibited more complex morphologies, mainly due to the formation of twinning.[4] Further experiments were carried out on NT samples where the surrounding SiO 2 layer was removed. The GaAs turned out to nucleate along specific crystallographic directions on such NTs. This observation can be explained by a simple model (Figure 69c) of nano- facet dependent growth kinetics, and was validated by HR-TEM analyses and found to agree with the nucleation behaviour on micron- sized substrate features.[5] Other alternatives to further increase the homogeneity of the size distribution and to reduce the defect density of the GaAs nuclei, a homogeneous array of Ga droplets was first produced on the Si NTs (Figure 69d), and then crystallized under an As flow at high temperature (Figure 69e–f). This resulted in a much narrower size distribution of the nuclei and in a reduction of the defect density. The results pave the way towards the integration of novel optoelectronic devices on the Si platform.

Figure 69. Side (a) and top (b) view NTs, (c) Facet selective nucleation, (d) Site controlled Ga droplet nucleation and (inset) single Ga droplet (e-f) GaAs on Si nanoheteroepitaxy by Ga droplets and (inset) HRTEM analysis of the resulting nano-crystals

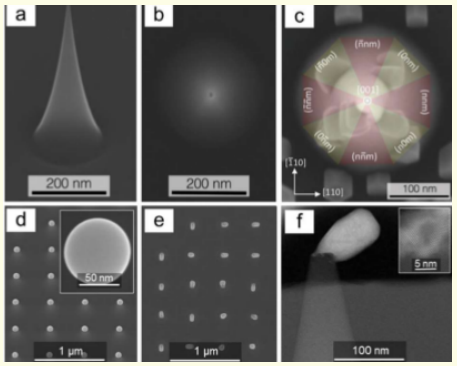

References

[1] Biegelsen, D.; Ponce, F.; Smith, A.; Tramontana, J. *Journal of applied physics* **1987**, *61*, 1856–1859.

[2] Glas, F. *Physical Review B* **2006**, *74*, 121302.

[3] others„ et al. *Nanotechnology* **2017**, *28*, 135701.

[4] Skibitzki, O.; Prieto, I.; Kozak, R.; Capellini, G.; Zaumseil, P.; Dasilva, Y. A. R.; Rossell, M. D.; Erni, R.; von Känel, H.; Schroeder, T. *Nanotechnology* **2017**, *28*, 135301.

[5] Prieto, I.; Kozak, R.; Skibitzki, O.; Rossell, M. D.; Schroeder, T.; Erni, R.; Von Känel, H. *small* **2017**, *13*, 1603122.

Ordering, Instabilities and Textures in Graphene Based Liquid Crystalline phases

Camilo Zamora-Ledezma[1,2]
Haifa Jeridi[3], Ty Phou[3], Eric Anglaret [3], and Christophe Blanc [3]
[1] *Yachay Tech University, School of Physical Sciences and Nanotechnology, 100115 Urcuquí, Ecuador*
[2] *Laboratorio De Física De La Materia Condensada, Centro De Física, Instituto Venezolano de Investigaciones Científícas, Altos De Pipe, 1204 Caracas, Venezuela*
[3] *Laboratoire Charles Coulomb UMR 5221, Université Montpellier, place Eugène Bataillon, 34095 Montpellier Cedex 5, France*
camilza@hotmail.com

To date, aqueous stable graphene flakes solutions can be obtained by simple REDOX reactions.[1–5] Most of the current applications regarding graphene require ordered nanostructured composites materials. Liquid crystal phases ordering represent an opportunity to arrange them into macroscopic assemblies with long-range ordering.[1,2] Preparing organized materials and thin films from these dispersions then requires a good control of the liquid crystal ordering during the deposition and the drying of the films. As a matter of fact, it turns out that graphene flakes easily align at high shear.[3,4] On the other hand, Graphene Flakes Liquid Crystals (GFLC) exhibit a very interesting behaviour at low shear or under small displacements, thin films often shows peculiar patterns (such as the periodic textures shown in Fig.70-70). We have shown how to create and stabilize large-sized periodic textures in GFLC. The patterns have been characterized under optical and electronic microscopies. Their stability can be explained by the competition between the anchoring field of the substrate and the presence of a yield stress resulting from the peculiar elastic and rheological properties of the GFLC. Our findings also clarify why long-standing hypotheses on the presence of exotic phases[1] at large concentrations are present in the literature.

Figure 70. Typical cross-polarized picture of organization in Graphene Liquid Crystal. Scale 700μm x 1mm.

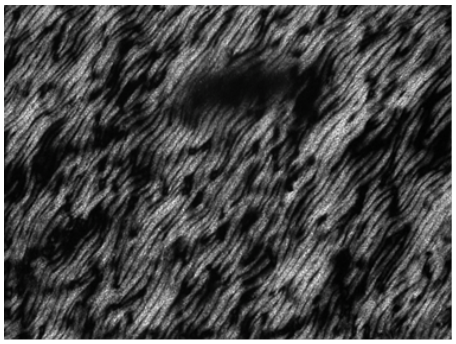

Figure 71. Typical Scanning Electron Microscopy picture of organization in Graphene Liquid Crystal. Scale bar 200 μm.

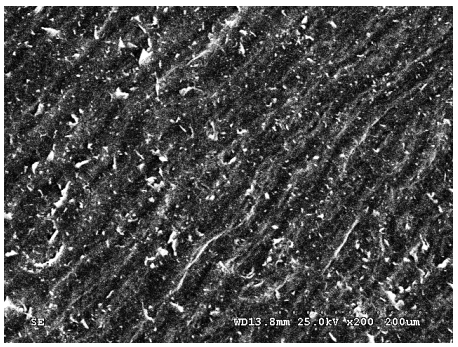

References

[1] Zakri, C.; Blanc, C.; Grelet, E.; Zamora-Ledezma, C.; Puech, N.; Anglaret, E.; Poulin, P. *Philosophical Transactions of the Royal Society A: Mathematical, Physical and Engineering Sciences* **2013**, *371*, 20120499.

[2] Zamora-Ledezma, C.; Puech, N.; Zakri, C.; Grelet, E.; Moulton, S. E.; Wallace, G. G.; Gambhir, S.; Blanc, C.; Anglaret, E.; Poulin, P. *The journal of physical chemistry letters* **2012**, *3*, 2425–2430.

[3] Poulin, P.; Jalili, R.; Neri, W.; Nallet, F.; Divoux, T.; Colin, A.; Aboutalebi, S. H.; Wallace, G.; Zakri, C. *Proceedings of the National Academy of Sciences* **2016**, *113*, 11088–11093.

[4] Zamora-Ledezma, C.; Jeridi, H.; Anglaret, E.; Blanc, C. Orientations and periodic textures in graphene liquid crystals. 27th International Liquid Crystal Conference (ILCC2018). 2018.

[5] Xu, Z.; Gao, C. *Nature communications* **2011**, *2*, 571.

Intrinsic Rashba Coupling due to Hydrogen bonding in DNA

Ernesto Medina
Solmar Varela, Barbara Montañes[1], Bertrand Berche[2], and Floralba López
Yachay Tech University, School of Physical Sciences and Nanotechnology and School of Chemistry and Engineering, 100119 Urcuquí, Ecuador
[1] *Centro de Física, Instituto Venezolano de Investigaciones Científicas, Caracas 1020A, Venezuela.*
[2] *Laboratoire de Physique et Chimie Théorique, UMR Université de Lorraine-CNRS 7019 54506 Vandoeuvre Les Nancy, France*
emedina@yachaytech.edu.ec

Chiraly induced spin selectivity (CISS) exhibited experimentally by chiral organic molecules such as Aminoacids, peptides and DNA among others,[1] is an outstanding spin polarizing mechanism that occurs in the absence of magnetic centers or heavy impurities. The essential ingredients to CISS are chirality and the spin-orbit coupling which enforces a time reversal symmetric Hamiltonian only broken by an external bias or dephasing processes. Analytical and numerical modeling of the effect, while having identified the correct symmetries,[2] have not fully determined the source of the spin-orbit coupling required to quantitatively explain the experimental data. In this work, we propose that the source of the strong spin activity is derived from an intrinsic Rash coupling due to the effect of the highly polarized Hydrogen bonds holding together the base pairs in DNA (see Fig. 72). Such polarized bridges produce electric fields in excess of 50GV/m[3] from which a Rashba coupling, involving Nitrogen and Oxygen atomic spin-orbit interactions, of ∼100 meV can be derived. The same coupling can be obtained for oligopeptides, whose helical structure is held in place by hydrogen bonding.
The model is proposed to be tested by using mechanical means to modulate the hydrogen bond polarization connected to the spin filtering strength(see Fig. 73).

Figure 72. Dipole moments associated with hydrogen bonds in the A-T base pair

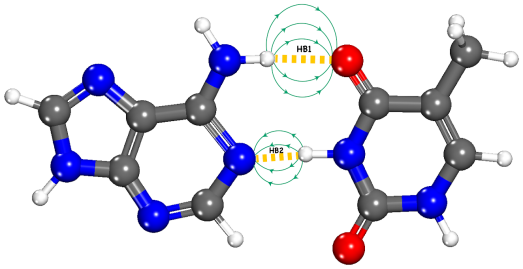

Figure 73. Rashba coupling as a function of when DNA is stretched holding both strands at each end.

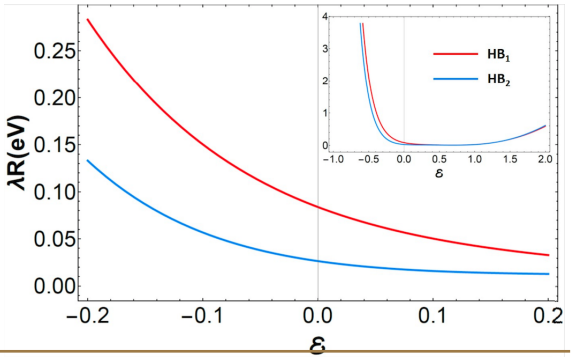

References

[1] Naaman, R.; Waldeck, D. H. *Annual review of physical chemistry* **2015**, *66*, 263–281.

[2] Varela, S.; Mujica, V.; Medina, E. *Physical Review B* **2016**, *93*, 155436.

[3] Ruiz-Blanco, Y.; Almeida, Y.; Sotomayor-Torres, C.; García, Y. *PloS one* **2017**, *12*, e0185638.

Index